VLBI DSN Flux Density Observations From 1989 to 1996 of 290 Extragalactic Radio Sources

R. F. Coker and C. S. Jacobs
Tracking Systems and Applications Section

L. E. Iriks
Allied Signal Corporation, Pasadena, California

Over the last 7 years, more than 35,000 correlated flux density observations, accurate to ∼20 percent, of 290 extragalactic radio sources have been conducted at S-band (2.3 GHz) and X-band (8.4 GHz) using the MkIII very long baseline interferometry (VLBI) system of the Deep Space Network (DSN). These ongoing observations, with typical 5σ detection limits of ∼45 mJy at S-band and ∼30 mJy at X-band, have been taken as part of the high-accuracy reference frame catalog required for the VLBI tracking of Galileo, Cassini, and future missions. A total flux density catalog, also accurate to ∼20 percent, with 1440 observations on 190 sources and typical detection limits of 0.8 Jy at S-band and 0.4 Jy at X-band, also has been created. We present here summary tables of these observations and discuss a few examples of variable sources.

I. Introduction

In order to provide a reference frame for angular tracking measurements of interplanetary spacecraft, a highly accurate astrometric catalog of compact extragalactic radio sources (generically, albeit somewhat inaccurately, referred to as quasars) is produced and maintained using very long baseline interferometry (VLBI) MkIII [1] observations taken with NASA's Deep Space Network (DSN) [2].[1] These "catalog experiments" are designed to use the DSN antennas at X-band (8.4 GHz) and S-band (2.3 GHz) to develop the astrometric catalog, but navigational scheduling also requires a priori knowledge regarding which antennas are needed to observe, with a signal-to-noise ratio (SNR) adequate for detection, a specific quasar on a specific baseline. Since the correlated flux density of a given quasar can change from month to month by as much as 50 percent in extreme cases, particularly at higher observing frequencies such as X-band [3], a method has been developed [4] that uses catalog experiments to easily and quickly produce a correlated and total flux density catalog that is accurate enough (∼20 percent) to determine which antenna pairs will be able to detect specified reference sources while providing valuable time and source

[1] There are plans for an article entitled "The JPL Extragalactic Radio Reference Frame: Astrometric Results of 1978–1996 Deep Space Network VLBI," by C. S. Jacobs, O. J. Sovers, C. J. Naudet, R. P. Branson, and R. F. Coker, to appear in the next issue of this publication, *The Telecommunications and Data Acquisition Progress Report 42-132, October–December 1997*, to be published on February 15, 1998.

structure variability information. The results of these flux density observations are presented here; the astrometric results will be presented elsewhere.[2]

It is hoped that the astronomical community will find this flux database of general use in identifying and analyzing such processes as extreme scattering events (ESEs) and the evolution of active galactic nuclei (AGN).

II. Observations and Data Reduction

At a rate of approximately one a month, from July 1989 to May 1996, 108 successful observing sessions involving either the Goldstone, California, to Madrid, Spain, baseline (8.4×10^3 km long) or the Goldstone to Tidbinbilla, Australia, baseline (10.6×10^3 km long) have been conducted, with data taken at S- and X-bands simultaneously to correct for charged-particle effects. The resulting fringe spacing is ∼3 milliarcseconds (mas) at S-band and ∼1 mas at X-band. The 290 detected sources are north of −45 deg declination but are otherwise fairly uniformly distributed all across the sky except for some clustering near the ecliptic, which was done intentionally to support spacecraft navigation. The data were recorded using the MkIII VLBI recording system in right-circular polarization [1] with a recorded bandwidth of 10 MHz spanning the 100-MHz bandpass at S-band and 18 MHz spanning the 400-MHz bandpass at X-band, while the Caltech/JPL Block II processor [5] has been used for correlating. Post-correlator processing is done using the programs FIT [8] and CFLUXES [4]. Future observations will be recorded using the MkIV system. Some of the early experiments used 70-meter antennas (DSS 14, DSS 43, or DSS 63), but most sessions used two high-efficiency (HEF) 34-meter antennas (DSS 15, DSS 45, or DSS 65).

System temperatures are measured using a broadband strip chart or power meter; in the absence of such data, system temperatures are modeled using an empirically determined mapping function (see [4] and references cited therein). Source temperatures are measured using a variant of the on–off technique; the resulting total flux density detection limits of 0.8 Jansky (Jy $\equiv 10^{-26}\,\mathrm{Watts/\,m^2/\,Hz}$) at S-band and 0.4 Jy at X-band (for the 34-meter HEF antennas) are due to the finite resolution of the system temperature measurements (0.01 dBm or usually ∼0.1 K), while the accuracy is limited to ∼20 percent by uncertainties in the antenna gain. Antenna gains are calculated based on approximate knowledge of the total flux densities of some sources and experimentally determined nominal antenna sensitivities [6,7]. Systematic calibration errors in system temperatures and antenna gains (e.g., a long-term temporal drift in gain) are the dominant error sources, limiting the flux accuracy for an experiment using two 34-meter HEF antennas to ∼10–20 percent. The correlated flux density detection limits, corresponding to a correlation amplitude SNR of 5 for an observation using two 34-meter HEF antennas, are ∼45 mJy at S-band and ∼30 mJy at X-band for a typical 150-second coherent integration. The detection limits for the 70-m antennas are correspondingly lower. The median source position accuracy is ∼0.2 mas, while the positions of rarely observed sources are accurate to within a few mas.[3] Details of standard radio reference frame experiments [2] and subsequent data reduction [5,8] can be found elsewhere.

III. Summary of Results

S-band correlated flux densities, in Janskys, for 290 extragalactic radio sources are presented in Table 1 in order of increasing right ascension (RA). The name of the source, as given in the JPL astrometric catalog [2],[4] is in the first column. In columns 2, 3, 4, 5, and 6 are the average correlated flux density, $\overline{S_{corr}}$; the rms variation of the observations, σ_{rms}; the minimum observed correlated flux density, S_{min}; the maximum observed correlated flux density, S_{max}; and the number of observations for that source for the

[2] Ibid.

[3] Ibid.

[4] Ibid.

Goldstone–Tidbinbilla baseline, N_{obs}, respectively. Columns 7 through 11 are the equivalent values for the Goldstone–Madrid baseline. Table 2 lists the X-band results.

A measure of source variability can be derived by comparing the minimum and maximum values in the tables to the expected errors of 10–20 percent. As is evident from Tables 1 and 2, most sources have a high degree of variability, due to either resolved source structure on the order of a few milliarcseconds or more in size or intrinsic temporal changes in the core of the source. Note that precision within a single experiment generally is better than ∼10 percent; as noted above, interexperiment systematic errors dominate the observational errors.

Total flux density results, also in Janskys, are presented in Table 3 for 190 sources in order of increasing RA. At X-band, 188 sources have been detected, while at S-band, only 67 sources have measurements at this time. The name of the source is in the first column. Columns 2, 3, 4, 5, and 6 are the average total flux density, $\overline{S_{tot}}$; the rms variation of the observations, σ_{rms}; the minimum observed flux density, S_{min}; the maximum observed flux density, S_{max}; and the number of observations for that source at X-band, N_{obs}, respectively. Columns 7 through 11 list the equivalent values for S-band. Since the sensitivity of the 34-meter HEF antennas is ∼0.25 K/Jy at X-band and ∼0.2 K/Jy at S-band and most sources have total flux densities on the order of a Jansky, it is often difficult to get reliable total flux density measurements, particularly with the presence of atmospheric fluctuations.

IV. Discussion

Although correlated flux densities on two baselines on a monthly basis can give little source structure detail, the cause of a source's variability sometimes can be determined and used as a guideline for more detailed observations with many baselines. For example, on the Goldstone–Madrid baseline, which is nearly east–west, the projected baseline length is nearly constant when observing high declination (>60-deg) sources, so as the baseline sweeps around in hour angle, the interferometer is sensitive to different parts of a source but with the same resolution. Figure 1 shows a plot of the S-band correlated flux density versus interferometer hour angle (IHA) for the circumpolar source 3C 371 (also known as 1807+698), which, due to its high declination, is visible only on the Goldstone–Madrid baseline. At a given IHA, this source shows little systematic temporal variation at S-band. However, the observed correlated flux

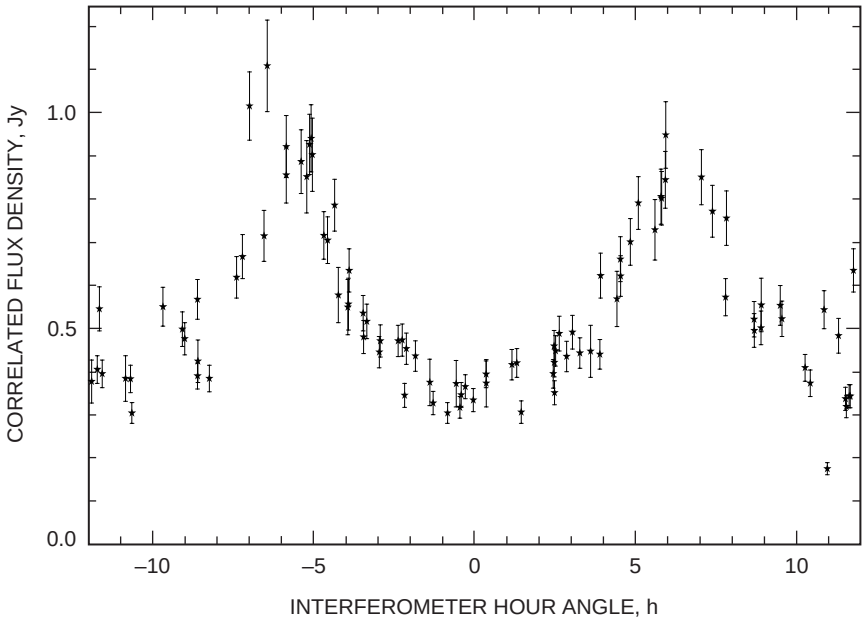

Fig. 1. S-band correlated flux density versus IHA for 3C 371.

density changes by more than a factor of 5 from ∼0.2 Jy to ∼1.1 Jy as the baseline rotates around the source. Also, since the total S-band flux density of 3C 371 is ∼3 Jy, the source clearly is highly resolved and extended. In particular, 3C 371 seems to be a temporally stable source that is much more extended along a position angle of ±90 deg (more than the resolution of ∼3 mas) than in the north–south direction. At X-band, the source is less temporally stable, but the east–west elongation still is visible. This is in agreement with published maps and models of this source that consist of a core with an extended east–west jet [9].

Another highly variable source is P 0735+17, whose correlated flux density varies by more than a factor of 10. Figure 2 shows a plot of X-band correlated flux density versus time for this source; Fig. 3 is of S-band. There is little correlation with IHA, so variability is temporal rather than structural. Indeed, since both baselines and both bands track the outburst and subsequent fading of this source (with S-band lagging X-band by ∼6 months), while the total flux density (∼3 Jy) does not, it is consistent with published maps [10] that show superluminal motion and rapid evolution of components not fully resolved on these baselines.

The compact source P 1741−038 underwent an ESE in 1992, resulting in a decrease in S-band flux of more than a factor of 2 that lasted for months. At X-band, the flux decrease of ∼20 percent is only marginally apparent. These results match published light curves for this event [11]. Although the structure of the source adds noise to the time series, particularly at the higher resolution of X-band, the catalog developed here can be used to identify and confirm ESEs that occur in the light curves of P 1741−038 and other sources.

V. Conclusion

As more reference frame catalog experiments are analyzed, this flux density database will continue to grow and to be used, for some sources at least, to create evolution and simplistic structure models. In the near future, flux data from more than 10 years of TEMPO experiments (see, e.g., [12]), with lower detection limits, are going to be added to the catalog, nearly doubling the number of observations. Additionally, as the Block V system and the MkIV format are installed in the DSN, the flux catalog accuracy and detection limits should improve by at least a factor of 2.

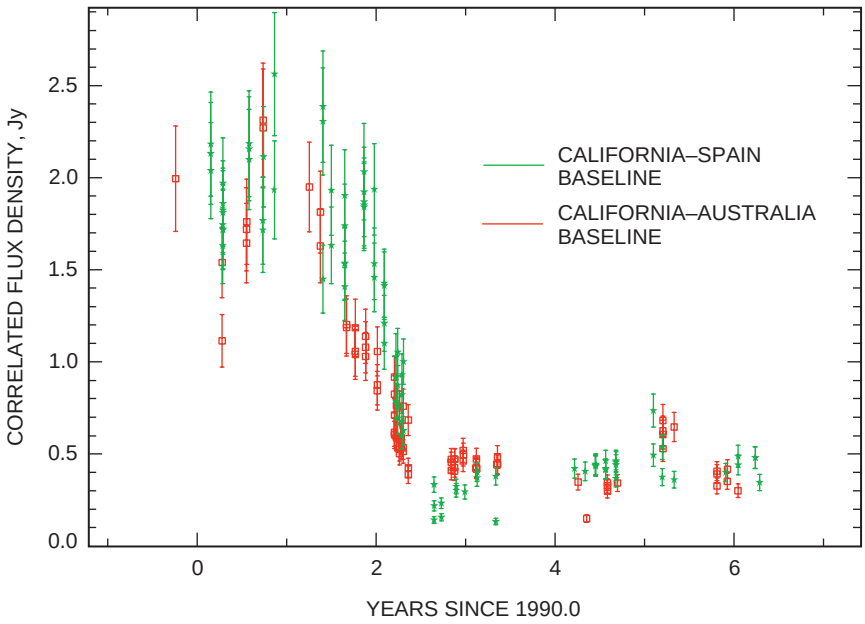

Fig. 2. X-band correlated flux density versus time for P 0735+17.

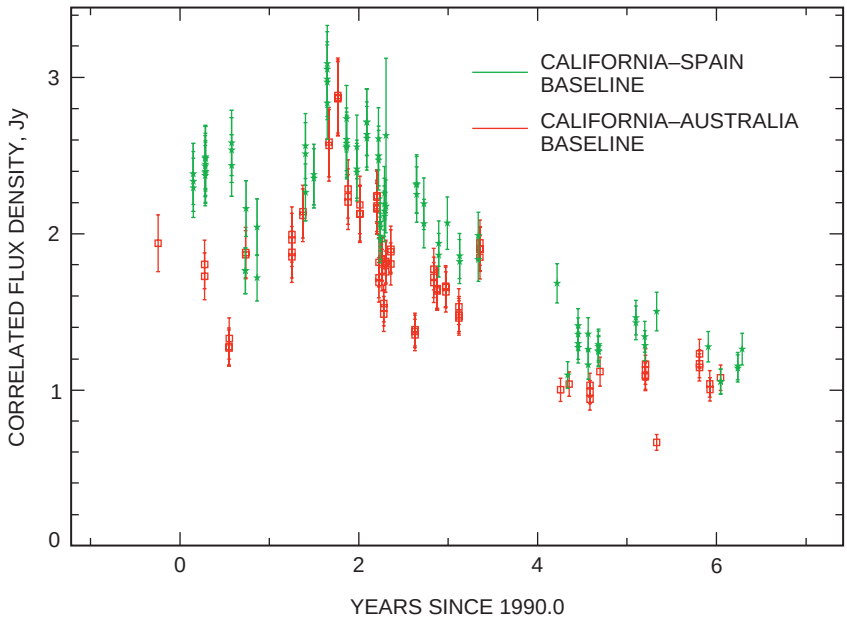

Fig. 3. S-band correlated flux density versus time for P 0735+17.

Acknowledgments

Many people were of assistance in this work. In particular, we would like to thank the personnel of the DSN for performing these sometimes-nonoperational observations, O. Sovers and C. Naudet for useful discussions, and P. Gorham for pointing out the ESE.

References

[1] A. E. E. Rogers and T. A. Clark, *Mark III Data Acquisition Terminal*, Crustal Dynamics Project, Goddard Space Flight Center, Greenbelt, Maryland, January 1982.

[2] O. J. Sovers, C. D. Edwards, C. S. Jacobs, G. E. Lanyi, K. M. Liewer, and R. N. Treuhaft, "Astrometric Results of 1978–1985 Deep Space Network Radio Interferometry: The JPL 1987-1 Extragalactic Source Catalog," *The Astronomical Journal*, vol. 95, pp. 1647–1658, 1988.

[3] T. F. Haddock, H. D. Aller, and M. F. Aller, "Frequent Observations of Extragalactic Compact Sources at 24 GHz," *The Astronomical Journal*, vol. 93, pp. 1356–1367, February 10, 1987.

[4] R. F. Coker, "Correlated Flux Densities From VLBI Observations With the DSN," *The Telecommunications and Data Acquisition Progress Report 42-111,*

July–September 1992, Jet Propulsion Laboratory, Pasadena, California, pp. 118–128, November 15, 1992.

[5] J. B. Thomas, *Interferometry Theory for the Block II Processor*, JPL Publication 87-29, Jet Propulsion Laboratory, Pasadena, California, October 15, 1987.

[6] P. H. Richter and S. D. Slobin, "DSN 70-Meter Antenna X- and S-Band Calibration Part I: Gain Measurements," *The Telecommunications and Data Acquisition Progress Report 42-97, January–March 1989*, pp. 314–351, May 15, 1989.

[7] S. D. Slobin and P. H. Richter, "DSN 70-Meter Antenna X- and S-Band Calibration Part II: System Noise Temperature Measurements and Telecommunications Link Evaluation," *The Telecommunications and Data Acquisition Progress Report 42-97, January–March 1989*, pp. 352–366, May 15, 1989.

[8] S. T. Lowe, *Theory of Post Block II VLBI Observable Extraction*, JPL Publication 92-7, Jet Propulsion Laboratory, Pasadena, California, July 15, 1992.

[9] T. V. Cawthorne, J. F. C. Wardle, D. H. Roberts, D. C. Gabuzda, and L. F. Brown, " Milliarcsecond Polarization Structure of 24 Objects from the Pearson–Readhead Sample of Bright Extragalactic Radio Sources. I. The Images," *The Astrophysical Journal*, vol. 416, pp. 496–518, October 20, 1993.

[10] D. C. Gabuzda, J. F. C. Wardle, D. H. Roberts, M. F. Aller, and H. D. Aller, "Unusual Evolution in the VLBI Structure of 0735+178," *The Astrophysical Journal*, vol. 435, pp. 128–139, November 1, 1994.

[11] A. L. Fey, A. W. Clegg, and R. L. Fiedler, "VLBI Observations of Eight Extreme Scattering Event Sources: Milliarcsecond-Scale Structure," *The Astrophysical Journal*, vol. 468, pp. 543–555, September 10, 1996.

[12] J. A. Steppe, S. H. Oliveau, and O. J. Sovers, "Earth Rotation Parameters From DSN VLBI: 1994," *Earth Rotation, Reference Frames and Atmospheric Excitation Functions Submitted for the 1993 IERS Annual Report*, IERS Technical Note 17, P. Charlot, ed., pp. R19–R32, Observatoire de Paris, Paris, September 1994.

Table 1. Correlated flux densities at 2.3 GHz (S-band).

Source	Goldstone–Australia baseline					Goldstone–Madrid baseline				
	$\overline{S_{corr}}$	σ_{rms}	S_{min}	S_{max}	N_{obs}	$\overline{S_{corr}}$	σ_{rms}	S_{min}	S_{max}	N_{obs}
0003−066	1.33	0.37	0.88	2.20	62	0.97	0.29	0.60	1.53	44
GC 0007+17	0.74	0.15	0.48	0.93	20	0.66	0.08	0.52	0.75	15
P 0008−264	0.26	0.05	0.20	0.32	7	0.00	0.00	0.00	0.00	0
P 0013−00	0.61	0.17	0.39	0.90	55	0.79	0.19	0.41	0.97	14
0014+813	0.00	0.00	0.00	0.00	0	0.40	0.06	0.30	0.53	14
0016+731	0.00	0.00	0.00	0.00	0	0.95	0.32	0.35	1.58	74
P 0019+058	0.32	0.08	0.08	0.44	28	0.38	0.03	0.36	0.42	5
P 0048−09	0.76	0.15	0.44	1.24	52	0.64	0.10	0.42	0.82	21
P 0104−408	0.67	0.15	0.49	0.94	43	0.00	0.00	0.00	0.00	0
P 0106+01	0.67	0.48	0.07	1.65	59	0.84	0.27	0.31	1.44	59
P 0111+021	0.39	0.07	0.19	0.51	52	0.07	0.00	0.07	0.08	2
P 0112−017	1.03	0.15	0.74	1.52	69	0.94	0.13	0.39	1.41	68
P 0113−118	0.86	0.14	0.61	1.10	24	1.06	0.23	0.41	1.42	47
P 0119+11	0.59	0.13	0.38	0.80	41	0.87	0.21	0.41	1.39	64
GC 0119+04	0.95	0.17	0.54	1.16	32	0.90	0.19	0.60	1.14	29
DA 55	0.45	0.18	0.23	0.92	15	0.57	0.30	0.07	1.20	101
0146+056	0.96	0.10	0.80	1.22	29	0.98	0.06	0.94	1.02	2
P 0149+21	0.20	0.07	0.08	0.35	52	0.36	0.07	0.25	0.50	32
0159+723	0.00	0.00	0.00	0.00	0	0.22	0.04	0.15	0.31	32
P 0201+113	0.70	0.10	0.35	0.88	58	0.63	0.12	0.34	0.92	37
P 0202+14	0.79	0.46	0.07	1.78	75	1.02	0.48	0.22	1.91	75
DW 0202+31	0.23	0.06	0.13	0.40	45	0.42	0.05	0.31	0.48	9
0212+735	0.00	0.00	0.00	0.00	0	0.84	0.50	0.11	1.96	97
GC 0221+06	0.40	0.09	0.21	0.84	67	0.26	0.04	0.15	0.34	32
DW 0224+67	0.00	0.00	0.00	0.00	0	0.73	0.19	0.35	1.04	17
P 0229+13	0.77	0.08	0.54	0.97	76	0.88	0.12	0.38	1.16	73
CTD 20	1.21	0.42	0.27	2.13	84	1.57	0.50	0.62	3.19	91
GC 0235+16	1.46	0.71	0.28	2.99	70	1.49	0.51	0.54	3.03	61
GC 0237+04	0.79	0.08	0.61	0.90	20	0.66	0.08	0.52	0.74	7
P 0237−23	0.32	0.17	0.12	0.77	21	0.00	0.00	0.00	0.00	0
P 0238−084	0.06	0.00	0.06	0.06	2	0.00	0.00	0.00	0.00	0
OD 166	0.96	0.10	0.74	1.15	48	0.49	0.18	0.18	0.91	54
GC 0250+17	0.05	0.01	0.05	0.05	1	0.05	0.01	0.05	0.05	2
OD 094.7	0.29	0.05	0.16	0.39	30	0.67	0.04	0.65	0.70	2
0259+121	0.08	0.02	0.05	0.11	8	0.25	0.05	0.18	0.34	17
OE 400	0.58	0.13	0.41	0.92	37	0.71	0.28	0.19	1.68	97
0302+625	0.00	0.00	0.00	0.00	0	0.14	0.04	0.05	0.25	81
0306+102	0.40	0.16	0.08	0.69	49	0.25	0.03	0.21	0.29	4
0309+411	0.23	0.05	0.13	0.35	34	0.17	0.06	0.09	0.31	41
3C 84	0.88	0.45	0.26	1.43	7	2.17	0.83	0.76	4.50	32
P 0317+188	0.40	0.04	0.33	0.47	15	0.32	0.07	0.24	0.50	19
0326+277	0.24	0.07	0.12	0.44	42	0.27	0.04	0.25	0.34	4
P 0332−403	1.03	0.15	0.71	1.28	37	0.00	0.00	0.00	0.00	0

Table 1 (cont'd).

Source	Goldstone–Australia baseline					Goldstone–Madrid baseline				
	$\overline{S_{corr}}$	σ_{rms}	S_{min}	S_{max}	N_{obs}	$\overline{S_{corr}}$	σ_{rms}	S_{min}	S_{max}	N_{obs}
NRAO 140	0.82	0.27	0.45	1.40	23	0.41	0.28	0.19	1.16	20
CTA 26	1.36	0.17	1.22	1.66	6	1.57	0.37	1.01	2.42	42
0341+158	0.13	0.05	0.08	0.20	7	0.22	0.04	0.13	0.30	18
0342+147	0.31	0.07	0.19	0.42	35	0.30	0.03	0.27	0.34	4
CTD 26	0.16	0.07	0.07	0.30	16	0.18	0.07	0.04	0.30	38
P 0402−362	0.62	0.11	0.44	0.94	77	0.00	0.00	0.00	0.00	0
0405+305	0.00	0.00	0.00	0.00	0	0.09	0.02	0.07	0.10	2
0406−127	0.18	0.05	0.12	0.31	38	0.30	0.07	0.25	0.41	4
GC 0406+12	0.46	0.12	0.25	0.83	45	0.43	0.00	0.43	0.44	2
P 0420−01	1.84	0.60	0.50	3.63	89	2.68	0.52	1.49	3.86	68
VRO 41.04.01	0.00	0.00	0.00	0.00	0	0.45	0.15	0.20	0.59	6
P 0425+048	0.17	0.06	0.07	0.34	34	0.00	0.00	0.00	0.00	0
3C 120	0.79	0.36	0.28	1.47	15	0.76	0.31	0.38	1.25	17
P 0434−188	0.89	0.12	0.58	1.15	84	0.62	0.06	0.49	0.81	43
P 0438−43	1.03	0.11	0.84	1.25	19	0.00	0.00	0.00	0.00	0
NRAO 190	0.62	0.15	0.62	0.62	1	0.74	0.19	0.74	0.74	1
0440+345	0.73	0.13	0.54	1.17	26	1.02	0.20	0.90	1.26	3
P 0446+11	0.24	0.16	0.04	0.45	7	0.29	0.12	0.12	0.38	4
P 0451−28	0.70	0.17	0.38	1.10	19	0.00	0.00	0.00	0.00	0
0454−234	0.89	0.30	0.33	1.56	50	1.28	0.26	0.87	1.71	13
P 0458−02	1.38	0.24	1.08	2.06	40	1.59	0.34	0.98	2.14	19
P 0458+138	0.12	0.08	0.07	0.31	26	0.20	0.09	0.16	0.28	2
GC 0459+06	0.35	0.05	0.25	0.41	11	0.43	0.11	0.44	0.44	1
0500+019	0.87	0.08	0.66	0.98	15	0.28	0.04	0.25	0.31	2
P 0502+049	0.22	0.07	0.10	0.33	13	0.06	0.01	0.06	0.06	1
0454+844	0.00	0.00	0.00	0.00	0	0.34	0.07	0.13	0.50	133
P 0506+101	0.44	0.30	0.11	1.43	51	0.25	0.13	0.10	0.55	22
P 0507+17	0.20	0.08	0.06	0.36	45	0.17	0.02	0.16	0.19	3
P 0511−220	0.27	0.07	0.17	0.38	10	0.20	0.08	0.15	0.39	9
P 0528+134	0.49	0.18	0.12	1.21	81	1.10	0.25	0.39	1.86	74
P 0537−441	1.10	0.82	0.16	2.88	29	0.00	0.00	0.00	0.00	0
P 0537−158	0.06	0.02	0.05	0.09	6	0.21	0.03	0.17	0.25	5
0536+145	0.68	0.12	0.38	0.86	63	0.72	0.11	0.48	0.86	17
0544+273	0.14	0.08	0.06	0.30	29	0.11	0.06	0.05	0.16	3
DA 193	2.21	0.28	1.28	2.98	101	2.33	0.29	1.57	2.89	130
0556+238	0.32	0.20	0.14	0.99	41	0.49	0.12	0.35	0.77	19
0600+177	0.32	0.07	0.15	0.60	64	0.45	0.13	0.36	0.65	4
P 0605−08	0.46	0.15	0.36	0.87	18	0.61	0.14	0.35	0.95	38
P 0607−15	1.76	0.53	0.37	2.37	14	1.67	0.53	0.85	2.35	25
0611+131	0.11	0.08	0.06	0.29	15	0.22	0.08	0.15	0.34	7
0615+820	0.00	0.00	0.00	0.00	0	0.59	0.08	0.36	0.77	51
3C 166	0.40	0.06	0.29	0.50	34	0.33	0.06	0.28	0.38	3
P 0646−306	0.46	0.15	0.19	0.66	24	0.00	0.00	0.00	0.00	0

Table 1 (cont'd).

Source	Goldstone–Australia baseline					Goldstone–Madrid baseline				
	$\overline{S_{corr}}$	σ_{rms}	S_{min}	S_{max}	N_{obs}	$\overline{S_{corr}}$	σ_{rms}	S_{min}	S_{max}	N_{obs}
0650+371	0.64	0.11	0.38	0.80	38	0.82	0.15	0.42	1.08	71
0657+172	0.96	0.38	0.21	1.78	84	0.87	0.38	0.40	1.60	50
OI 417	0.38	0.14	0.13	0.57	16	0.68	0.27	0.20	1.06	15
0716+714	0.00	0.00	0.00	0.00	0	0.27	0.07	0.13	0.41	42
P 0722+145	0.51	0.05	0.41	0.58	8	0.43	0.04	0.38	0.47	4
DW 0723−00	0.49	0.11	0.29	0.67	22	0.34	0.00	0.34	0.34	2
P 0727−11	2.64	0.69	0.84	4.15	100	2.26	0.62	0.58	3.12	75
P 0735+17	1.69	0.47	0.66	2.88	83	2.05	0.55	1.05	3.09	90
P 0736+01	0.74	0.28	0.38	1.42	26	0.40	0.09	0.19	0.54	26
OI 363	1.97	0.73	1.22	2.62	3	1.93	0.15	1.69	2.11	6
DW 0742+10	0.83	0.09	0.63	1.00	22	2.57	0.11	2.38	2.75	16
P 0743−006	0.53	0.05	0.38	0.64	31	0.69	0.08	0.55	0.79	10
GC 0743+25	0.51	0.13	0.37	0.76	9	0.54	0.02	0.53	0.55	2
B2 0745+24	0.63	0.18	0.16	0.80	20	0.43	0.13	0.13	0.67	42
P 0748+126	0.77	0.11	0.60	0.95	17	0.56	0.09	0.45	0.73	11
0749+540	0.00	0.00	0.00	0.00	0	0.95	0.15	0.31	1.25	55
P 0754+100	0.36	0.08	0.26	0.49	6	0.89	0.10	0.82	0.96	2
P 0805−07	0.92	0.10	0.75	1.05	24	0.91	0.09	0.74	1.16	49
P 0808+019	0.73	0.19	0.45	1.20	43	0.78	0.19	0.41	1.22	34
OJ 425	0.65	0.10	0.39	0.86	63	0.65	0.12	0.33	0.88	49
P 0823+033	0.97	0.18	0.40	1.35	93	1.37	0.22	0.73	1.79	90
B2 0827+24	0.44	0.04	0.36	0.47	8	0.35	0.08	0.27	0.48	5
OJ 448	0.00	0.00	0.00	0.00	0	0.18	0.03	0.12	0.25	23
0833+585	0.00	0.00	0.00	0.00	0	0.41	0.18	0.05	0.60	32
OJ 287	1.17	0.35	0.40	1.98	91	1.41	0.39	0.42	2.22	99
P 0859−14	0.70	0.19	0.32	0.93	20	0.60	0.07	0.46	0.75	29
OJ 499	0.24	0.10	0.06	0.36	10	0.47	0.12	0.24	0.69	46
P 0906+01	0.31	0.02	0.27	0.34	14	0.27	0.02	0.25	0.28	2
P 0912+029	0.29	0.06	0.19	0.41	11	0.00	0.00	0.00	0.00	0
0917+449	0.52	0.11	0.28	0.70	33	0.93	0.12	0.52	1.15	69
0919−260	0.08	0.03	0.04	0.13	12	0.00	0.00	0.00	0.00	0
P 0920−39	0.12	0.08	0.05	0.29	17	0.00	0.00	0.00	0.00	0
4C 39.25	2.43	0.53	0.89	4.67	87	2.39	0.43	1.41	3.53	103
P 0925−203	0.17	0.10	0.05	0.32	9	0.44	0.03	0.42	0.48	4
AO 0952+17	0.12	0.04	0.05	0.17	15	0.32	0.13	0.17	0.49	7
OK 290	1.08	0.16	0.60	1.35	50	1.08	0.14	0.68	1.30	52
GC 1004+14	0.30	0.07	0.15	0.37	7	0.21	0.14	0.15	0.39	3
1011+250	0.22	0.05	0.11	0.28	19	0.24	0.05	0.16	0.43	37
1012+232	0.63	0.12	0.49	0.90	14	0.00	0.00	0.00	0.00	0
GC 1022+19	0.09	0.08	0.05	0.27	7	0.22	0.08	0.17	0.32	6
P 1034−293	0.85	0.31	0.38	2.37	99	0.00	0.00	0.00	0.00	0
OL 064.5	0.66	0.10	0.48	0.83	14	0.76	0.06	0.66	0.83	7
3C 245	0.33	0.14	0.16	0.43	3	0.29	0.09	0.15	0.34	4

Table 1 (cont'd).

Source	Goldstone–Australia baseline					Goldstone–Madrid baseline				
	$\overline{S_{corr}}$	σ_{rms}	S_{min}	S_{max}	N_{obs}	$\overline{S_{corr}}$	σ_{rms}	S_{min}	S_{max}	N_{obs}
1039+811	0.00	0.00	0.00	0.00	0	0.56	0.16	0.34	0.90	76
P 1042+071	0.19	0.08	0.08	0.27	4	0.16	0.10	0.10	0.33	7
1044+719	0.00	0.00	0.00	0.00	0	0.93	0.18	0.70	1.33	40
P 1055+01	1.19	0.18	0.83	1.73	94	0.66	0.15	0.41	1.02	76
P 1104−445	0.48	0.21	0.13	1.18	30	0.00	0.00	0.00	0.00	0
GC 1111+14	0.47	0.06	0.40	0.57	7	0.49	0.02	0.47	0.50	2
P 1116+12	0.46	0.06	0.36	0.54	16	0.63	0.04	0.55	0.69	25
P 1123+26	0.83	0.10	0.62	1.13	63	0.81	0.09	0.47	1.01	102
P 1124−186	0.50	0.13	0.27	0.68	26	0.52	0.15	0.37	0.84	10
P 1127−14	1.12	0.23	0.58	1.38	15	1.53	0.25	0.83	2.00	43
GC 1128+38	0.45	0.15	0.37	0.85	14	0.68	0.06	0.63	0.75	3
P 1130+009	0.35	0.08	0.21	0.47	19	0.36	0.09	0.22	0.43	5
1144+402	0.22	0.10	0.10	0.37	22	0.32	0.04	0.25	0.38	12
P 1144−379	1.71	0.77	0.46	3.71	104	0.00	0.00	0.00	0.00	0
1145−071	0.44	0.09	0.36	0.67	11	0.41	0.10	0.14	0.48	10
P 1148−00	0.19	0.07	0.06	0.26	6	0.40	0.02	0.38	0.44	4
1150+812	0.00	0.00	0.00	0.00	0	0.70	0.20	0.33	1.30	84
P 1156−094	0.06	0.01	0.04	0.08	13	0.00	0.00	0.00	0.00	0
GC 1156+29	0.74	0.17	0.34	1.03	40	0.93	0.22	0.55	1.45	61
ON 231	0.26	0.16	0.09	0.83	35	0.29	0.12	0.07	0.47	13
P 1222+037	0.55	0.11	0.34	0.65	6	0.62	0.16	0.62	0.62	1
3C 273	1.99	0.94	0.32	4.59	77	3.91	1.84	0.71	7.06	70
3C 274	0.26	0.11	0.14	0.39	5	0.00	0.00	0.00	0.00	0
1243−072	0.17	0.08	0.08	0.27	8	0.09	0.08	0.06	0.32	10
P 1244−255	1.11	0.31	0.18	1.57	76	1.14	0.18	0.95	1.30	4
P 1252+11	0.27	0.08	0.10	0.35	21	0.19	0.04	0.10	0.29	22
3C 279	1.26	0.31	0.65	1.65	20	3.03	0.57	1.24	4.38	64
P 1302−102	0.41	0.12	0.23	0.66	28	0.72	0.10	0.57	0.92	38
B2 1308+32	1.30	0.61	0.39	2.74	87	1.28	0.74	0.31	3.24	108
OP−322	0.68	0.24	0.32	1.47	81	0.00	0.00	0.00	0.00	0
OP 326	0.17	0.04	0.10	0.29	29	0.17	0.06	0.06	0.29	19
1324+224	1.00	0.19	0.67	1.49	61	1.12	0.22	0.73	1.76	74
DW 1335−12	0.91	0.33	0.29	1.93	91	1.96	0.50	1.01	3.03	72
1338+381	0.25	0.02	0.23	0.27	4	0.29	0.05	0.21	0.35	11
GC 1342+662	0.00	0.00	0.00	0.00	0	0.15	0.08	0.10	0.30	8
GC 1342+663	0.00	0.00	0.00	0.00	0	0.57	0.08	0.29	0.80	95
P 1349−439	0.22	0.08	0.08	0.37	44	0.00	0.00	0.00	0.00	0
P 1354+19	0.72	0.19	0.39	1.39	80	0.44	0.19	0.15	1.38	85
OP−192	0.37	0.12	0.14	0.71	55	0.40	0.14	0.30	0.82	13
OQ 208	0.21	0.08	0.08	0.39	43	0.83	0.15	0.73	1.15	7
P 1406−076	0.22	0.08	0.07	0.37	38	0.15	0.10	0.12	0.32	4
P 1413+135	0.07	0.02	0.04	0.09	15	0.07	0.01	0.05	0.10	24
GC 1418+54	0.00	0.00	0.00	0.00	0	0.58	0.38	0.32	1.03	3

Table 1 (cont'd).

Source	Goldstone–Australia baseline					Goldstone–Madrid baseline				
	$\overline{S_{corr}}$	σ_{rms}	S_{min}	S_{max}	N_{obs}	$\overline{S_{corr}}$	σ_{rms}	S_{min}	S_{max}	N_{obs}
P1424−41	0.69	0.20	0.27	1.03	58	0.00	0.00	0.00	0.00	0
OQ−151	0.58	0.07	0.42	0.69	30	0.41	0.02	0.39	0.44	3
P 1435−218	0.41	0.12	0.17	0.62	34	0.44	0.09	0.20	0.52	11
1443−162	0.39	0.07	0.21	0.53	31	0.27	0.06	0.24	0.35	5
P 1445−16	0.49	0.14	0.22	0.99	45	0.63	0.20	0.47	0.93	6
OR 103	1.06	0.18	0.72	1.79	91	0.94	0.17	0.56	1.74	82
1504+377	0.18	0.08	0.10	0.26	7	0.34	0.12	0.15	0.54	24
P 1504−167	0.78	0.33	0.11	1.47	63	1.66	0.31	0.65	2.13	49
P 1510−08	1.82	0.49	0.44	2.75	87	1.62	0.50	0.51	2.45	71
P 1511−100	0.72	0.17	0.37	1.01	33	0.80	0.07	0.71	0.89	8
P 1514−24	0.67	0.33	0.17	1.32	46	0.73	0.18	0.73	0.73	1
P 1519−273	1.27	0.32	0.48	1.87	82	0.00	0.00	0.00	0.00	0
P 1532+01	0.68	0.12	0.54	1.05	20	0.59	0.04	0.51	0.64	21
GC 1538+14	0.42	0.08	0.28	0.57	53	0.40	0.07	0.27	0.52	30
P 1546+027	0.39	0.07	0.29	0.46	13	0.58	0.18	0.28	0.90	36
DW 1548+05	0.68	0.14	0.45	0.89	23	1.15	0.17	0.87	1.77	45
DW 1555+00	0.95	0.24	0.55	1.42	77	1.00	0.25	0.51	1.37	71
P 1555−140	0.11	0.03	0.06	0.15	8	0.00	0.00	0.00	0.00	0
B2 1600+33	0.86	0.12	0.74	1.05	5	1.87	0.16	1.51	2.22	27
P 1604−333	0.19	0.03	0.14	0.30	43	0.00	0.00	0.00	0.00	0
P 1606+10	1.20	0.09	1.06	1.44	33	0.95	0.10	0.85	1.05	5
DA 406	0.76	0.30	0.29	1.22	21	1.45	0.42	0.79	2.63	80
P 1614+051	0.36	0.05	0.30	0.43	6	0.56	0.06	0.49	0.65	7
P 1622−253	0.41	0.26	0.04	1.28	25	0.00	0.00	0.00	0.00	0
1624+416	0.36	0.05	0.27	0.46	33	0.45	0.12	0.19	0.66	11
P 1622−29	0.37	0.17	0.07	0.79	25	0.00	0.00	0.00	0.00	0
GC 1633+38	1.73	0.15	1.51	1.89	8	1.47	0.23	0.73	2.07	90
P 1637+574	0.00	0.00	0.00	0.00	0	0.77	0.23	0.32	1.30	120
NRAO 512	1.10	0.08	1.02	1.17	4	0.99	0.19	0.47	1.44	67
1642+690	0.00	0.00	0.00	0.00	0	0.52	0.25	0.16	1.10	75
3C 345	1.13	0.94	0.11	5.64	85	1.32	0.78	0.16	2.96	84
P 1647−296	0.36	0.20	0.07	0.67	26	0.00	0.00	0.00	0.00	0
DA 426	0.42	0.09	0.19	0.57	20	0.37	0.07	0.27	0.48	11
OS 092	0.52	0.14	0.33	0.85	12	0.25	0.08	0.14	0.40	16
DW 1656+05	0.65	0.06	0.51	0.73	13	0.64	0.06	0.51	0.75	24
P 1657−261	0.83	0.44	0.12	1.97	70	0.95	0.02	0.94	0.97	2
OT−111	0.16	0.06	0.06	0.28	49	0.31	0.05	0.20	0.40	17
GC 1717+17	0.44	0.11	0.44	0.44	1	0.66	0.02	0.65	0.68	2
NRAO 530	0.50	0.24	0.11	1.21	105	2.03	0.88	0.40	3.57	69
1732+389	0.87	0.16	0.42	1.21	53	0.90	0.20	0.34	1.31	61
OT 465	0.56	0.13	0.42	0.69	5	0.58	0.27	0.33	1.06	10
4C 51.37	0.00	0.00	0.00	0.00	0	1.37	0.75	0.12	2.63	99
P 1741−038	1.35	0.21	0.68	1.87	102	1.70	0.27	0.86	2.65	79

Table 1 (cont'd).

Source	Goldstone–Australia baseline					Goldstone–Madrid baseline				
	$\overline{S_{corr}}$	σ_{rms}	S_{min}	S_{max}	N_{obs}	$\overline{S_{corr}}$	σ_{rms}	S_{min}	S_{max}	N_{obs}
GC 1743+17	0.47	0.05	0.34	0.53	14	0.57	0.11	0.43	0.85	51
OT 081	0.41	0.06	0.28	0.54	28	0.79	0.18	0.41	1.19	80
GC 1751+28	0.21	0.08	0.10	0.34	25	0.39	0.02	0.36	0.42	8
1803+784	0.00	0.00	0.00	0.00	0	1.25	0.37	0.55	2.34	112
3C 371	0.00	0.00	0.00	0.00	0	0.55	0.19	0.17	1.11	98
1826+796	0.00	0.00	0.00	0.00	0	0.15	0.05	0.07	0.25	24
P 1821+10	0.83	0.21	0.63	1.11	4	0.80	0.13	0.59	0.91	5
3C 390.3	0.00	0.00	0.00	0.00	0	0.19	0.09	0.09	0.36	12
3C 395	1.22	0.31	0.77	1.64	12	1.12	0.40	0.65	1.95	11
OV−213	0.68	0.26	0.07	1.29	88	1.06	0.37	0.35	1.64	29
OV−235	1.77	0.50	0.57	2.77	97	2.00	0.48	0.59	2.71	26
OV−236	2.91	1.41	0.30	6.18	116	0.00	0.00	0.00	0.00	0
OV 239.7	0.22	0.13	0.09	0.84	77	0.33	0.11	0.08	0.69	97
1928+738	0.00	0.00	0.00	0.00	0	1.26	0.59	0.29	2.87	90
1929+226	0.25	0.03	0.20	0.29	5	0.29	0.06	0.15	0.39	18
P 1933−400	0.50	0.09	0.36	0.72	77	0.00	0.00	0.00	0.00	0
P 1936−15	0.37	0.10	0.08	0.60	46	0.48	0.02	0.46	0.50	4
1947+079	0.36	0.15	0.14	0.64	15	0.70	0.19	0.30	0.91	8
1954+513	0.00	0.00	0.00	0.00	0	0.73	0.13	0.51	0.95	91
1955+335	0.00	0.00	0.00	0.00	0	0.01	0.00	0.01	0.01	1
OV−198	1.12	0.49	0.07	2.48	106	1.11	0.59	0.18	2.13	48
OW−015	0.50	0.07	0.40	0.67	20	0.00	0.00	0.00	0.00	0
P 2008−159	0.36	0.13	0.22	0.82	51	0.65	0.12	0.54	1.09	21
2017+743	0.00	0.00	0.00	0.00	0	0.19	0.04	0.12	0.32	36
OW 637	0.00	0.00	0.00	0.00	0	0.54	0.28	0.11	1.35	61
2021+317	0.08	0.02	0.06	0.11	4	0.26	0.08	0.13	0.43	31
OW 551	0.00	0.00	0.00	0.00	0	0.68	0.25	0.35	0.79	3
P 2029+121	0.40	0.06	0.33	0.45	3	0.50	0.04	0.47	0.53	2
3C 418	0.00	0.00	0.00	0.00	0	0.66	0.29	0.12	1.52	35
2051+745	0.00	0.00	0.00	0.00	0	0.18	0.07	0.09	0.35	22
2100+468	0.00	0.00	0.00	0.00	0	0.01	0.00	0.00	0.01	6
P 2106−413	1.10	0.19	0.76	1.42	22	0.00	0.00	0.00	0.00	0
B2 2113+29B	0.41	0.04	0.38	0.45	4	0.56	0.18	0.28	0.90	35
OX 036	1.63	0.57	0.68	3.18	46	1.96	0.64	0.58	3.08	13
P 2126−15	0.14	0.07	0.05	0.30	24	0.78	0.09	0.60	0.94	12
P 2127+04	0.52	0.10	0.42	0.69	7	0.26	0.07	0.19	0.37	8
P 2128−12	0.47	0.14	0.31	0.91	46	0.90	0.46	0.31	2.43	23
P 2131−021	0.84	0.31	0.34	1.38	76	0.83	0.34	0.33	1.43	57
P 2134+004	0.92	0.22	0.57	1.56	89	2.70	0.27	1.98	3.34	62
OX 161	0.44	0.07	0.34	0.56	8	0.70	0.10	0.54	0.86	14
OX−173	0.23	0.11	0.07	0.38	26	0.19	0.05	0.14	0.32	11
OX 074	0.71	0.18	0.48	1.04	15	0.97	0.17	0.79	1.25	7
P2145+06	1.66	0.25	1.10	2.16	73	1.34	0.25	0.62	2.14	70

Table 1 (cont'd).

Source	Goldstone–Australia baseline					Goldstone–Madrid baseline				
	$\overline{S_{corr}}$	σ_{rms}	S_{min}	S_{max}	N_{obs}	$\overline{S_{corr}}$	σ_{rms}	S_{min}	S_{max}	N_{obs}
OX 082	0.62	0.05	0.50	0.71	36	0.65	0.02	0.60	0.67	7
2150+173	0.25	0.09	0.06	0.37	11	0.23	0.04	0.17	0.33	23
OX−192	1.46	0.23	0.53	1.97	37	1.42	0.15	1.13	1.74	33
VRO 42.22.01	0.54	0.35	0.08	1.59	71	1.46	1.03	0.19	5.72	112
B2 2201+31A	0.41	0.21	0.10	0.76	34	1.42	0.47	0.36	2.21	33
P 2216−03	0.92	0.13	0.63	1.11	51	1.85	0.21	1.53	2.28	32
3C 446	1.57	0.36	0.91	2.21	47	1.76	0.55	0.62	2.48	27
P 2227−08	0.66	0.21	0.37	1.11	60	0.91	0.28	0.53	1.31	19
2229+695	0.00	0.00	0.00	0.00	0	0.42	0.25	0.18	1.23	27
CTA 102	1.72	0.25	1.23	2.29	77	0.87	0.49	0.17	2.53	67
GC 2234+28	1.06	0.26	0.62	1.68	72	1.19	0.24	0.64	1.72	69
P 2233−148	0.27	0.04	0.19	0.32	24	0.12	0.06	0.09	0.31	11
OY−172.6	0.71	0.14	0.42	0.98	88	1.04	0.11	0.76	1.25	56
P 2245−328	0.42	0.15	0.21	1.04	90	0.00	0.00	0.00	0.00	0
3C 454.3	2.97	1.73	0.77	6.63	74	3.31	1.64	1.05	6.86	51
P 2252−089	0.13	0.06	0.04	0.29	26	0.07	0.02	0.05	0.10	9
GC 2253+41	0.56	0.19	0.20	0.91	28	0.00	0.00	0.00	0.00	0
GC 2254+07	0.12	0.06	0.06	0.26	21	0.11	0.10	0.05	0.28	10
P 2254+024	0.20	0.10	0.08	0.40	29	0.20	0.06	0.12	0.31	7
P 2255−282	0.60	0.06	0.47	0.73	50	0.00	0.00	0.00	0.00	0
GC 2318+04	0.49	0.18	0.27	0.98	44	0.33	0.12	0.16	0.64	20
B2 2319+27	0.08	0.01	0.06	0.09	4	0.41	0.07	0.29	0.50	20
P 2320−035	0.37	0.07	0.21	0.63	60	0.55	0.05	0.40	0.65	48
P 2328+10	0.77	0.10	0.59	0.90	24	0.66	0.06	0.58	0.74	7
2331−240	0.50	0.12	0.29	0.73	44	0.22	0.06	0.14	0.34	11
P 2335−027	0.19	0.07	0.06	0.29	29	0.26	0.07	0.12	0.35	22
P 2344+09	0.30	0.11	0.07	0.42	23	0.48	0.12	0.39	0.61	3
P 2345−16	1.89	0.31	0.78	2.77	83	1.04	0.36	0.35	1.80	44
2351+456	0.10	0.03	0.05	0.14	18	0.15	0.06	0.05	0.30	26
2351−154	0.53	0.11	0.26	0.73	41	0.61	0.12	0.32	0.76	24
DA 611	0.00	0.00	0.00	0.00	0	0.51	0.13	0.51	0.51	1
P 2355−106	0.68	0.13	0.40	0.97	68	0.77	0.12	0.57	1.02	25

Table 2. Correlated flux densities at 8.4 GHz (X-band).

Source	Goldstone–Australia baseline					Goldstone–Madrid baseline				
	$\overline{S_{corr}}$	σ_{rms}	S_{min}	S_{max}	N_{obs}	$\overline{S_{corr}}$	σ_{rms}	S_{min}	S_{max}	N_{obs}
0003−066	0.55	0.19	0.12	0.90	58	1.30	0.38	0.41	1.97	44
GC 0007+17	0.16	0.06	0.08	0.26	19	0.15	0.03	0.12	0.21	15
P 0008−264	0.21	0.07	0.12	0.28	7	0.00	0.00	0.00	0.00	0
P 0013−00	0.15	0.06	0.05	0.26	53	0.23	0.06	0.14	0.29	14
0014+813	0.00	0.00	0.00	0.00	0	0.64	0.14	0.37	0.91	14
0016+731	0.00	0.00	0.00	0.00	0	0.49	0.27	0.03	0.98	74
P 0019+058	0.20	0.06	0.09	0.39	28	0.19	0.06	0.12	0.25	5
P 0048−09	1.01	0.31	0.50	1.96	50	0.67	0.22	0.33	1.03	21
P 0104−408	2.09	0.71	1.18	4.04	43	0.00	0.00	0.00	0.00	0
P 0106+01	0.56	0.26	0.14	1.08	55	0.71	0.29	0.17	1.14	59
P 0111+021	0.40	0.07	0.10	0.51	51	0.14	0.02	0.13	0.16	2
P 0112−017	0.46	0.14	0.18	0.80	64	0.45	0.12	0.21	0.66	68
P 0113−118	0.61	0.19	0.25	0.95	24	0.37	0.13	0.10	0.62	47
P 0119+11	0.49	0.20	0.04	0.76	38	1.09	0.25	0.55	1.71	64
GC 0119+04	0.68	0.21	0.39	1.25	31	0.63	0.27	0.36	1.14	29
DA 55	0.62	0.48	0.19	1.59	15	0.72	0.39	0.27	2.35	101
0146+056	0.36	0.05	0.28	0.46	28	0.15	0.00	0.15	0.16	2
P 0149+21	0.45	0.12	0.27	0.85	52	0.60	0.13	0.36	1.03	32
0159+723	0.00	0.00	0.00	0.00	0	0.11	0.04	0.03	0.21	32
P 0201+113	0.30	0.11	0.11	0.58	54	0.35	0.11	0.20	0.55	37
P 0202+14	1.24	0.46	0.13	2.12	68	1.35	0.46	0.61	2.49	75
DW 0202+31	0.39	0.17	0.19	0.80	40	0.30	0.04	0.24	0.40	9
0212+735	0.00	0.00	0.00	0.00	0	1.03	0.40	0.30	2.18	97
GC 0221+06	0.61	0.17	0.25	1.17	65	0.42	0.10	0.28	0.68	32
DW 0224+67	0.00	0.00	0.00	0.00	0	0.87	0.71	0.09	2.22	17
P 0229+13	0.43	0.12	0.24	0.79	69	0.44	0.12	0.23	0.75	73
CTD 20	1.09	0.26	0.57	1.70	79	1.42	0.41	0.62	2.41	91
GC 0235+16	1.30	0.95	0.20	3.56	65	1.26	0.80	0.15	2.68	61
GC 0237+04	0.59	0.22	0.30	1.04	19	0.76	0.10	0.61	0.91	7
P 0237−23	0.08	0.03	0.04	0.18	20	0.00	0.00	0.00	0.00	0
P 0238−084	0.10	0.06	0.06	0.14	2	0.00	0.00	0.00	0.00	0
OD 166	0.57	0.16	0.36	0.87	45	0.49	0.12	0.26	0.84	54
GC 0250+17	0.03	0.01	0.03	0.03	1	0.05	0.02	0.03	0.06	2
OD 094.7	0.14	0.09	0.04	0.38	27	0.35	0.03	0.34	0.37	2
0259+121	0.05	0.01	0.04	0.07	8	0.08	0.05	0.04	0.21	17
OE 400	0.52	0.16	0.27	0.84	34	0.55	0.20	0.16	1.17	97
0302+625	0.00	0.00	0.00	0.00	0	0.10	0.04	0.04	0.22	81
0306+102	0.33	0.17	0.11	0.63	48	0.24	0.16	0.15	0.47	4
0309+411	0.31	0.05	0.19	0.40	32	0.25	0.06	0.07	0.38	41
3C 84	0.35	0.15	0.10	0.58	7	0.48	0.22	0.10	0.82	32
P 0317+188	0.20	0.04	0.10	0.23	15	0.23	0.04	0.16	0.29	19
0326+277	0.18	0.06	0.12	0.35	38	0.15	0.07	0.09	0.22	4
P 0332−403	1.23	0.46	0.43	2.31	37	0.00	0.00	0.00	0.00	0

Table 2 (cont'd).

Source	Goldstone–Australia baseline					Goldstone–Madrid baseline				
	$\overline{S_{corr}}$	σ_{rms}	S_{min}	S_{max}	N_{obs}	$\overline{S_{corr}}$	σ_{rms}	S_{min}	S_{max}	N_{obs}
NRAO 140	0.65	0.10	0.39	0.83	23	0.60	0.11	0.38	0.82	20
CTA 26	0.51	0.08	0.41	0.63	6	0.60	0.22	0.05	1.01	42
0341+158	0.05	0.02	0.04	0.09	7	0.12	0.05	0.04	0.24	18
0342+147	0.23	0.10	0.07	0.42	33	0.18	0.07	0.12	0.26	4
CTD 26	0.21	0.04	0.11	0.25	16	0.26	0.04	0.17	0.34	38
P 0402−362	1.09	0.24	0.31	1.40	71	0.00	0.00	0.00	0.00	0
0405+305	0.00	0.00	0.00	0.00	0	0.05	0.01	0.04	0.06	2
0406−127	0.14	0.05	0.09	0.29	37	0.19	0.06	0.14	0.27	4
GC 0406+12	0.33	0.08	0.11	0.48	43	0.19	0.00	0.19	0.20	2
P 0420−01	0.97	0.33	0.38	1.97	82	1.06	0.37	0.31	2.19	68
VRO 41.04.01	0.00	0.00	0.00	0.00	0	0.20	0.04	0.14	0.23	6
P 0425+048	0.14	0.04	0.07	0.26	34	0.00	0.00	0.00	0.00	0
3C 120	0.51	0.21	0.17	0.91	15	0.30	0.12	0.15	0.53	17
P 0434−188	0.52	0.11	0.27	0.74	76	0.35	0.09	0.11	0.48	43
P 0438−43	0.61	0.19	0.29	0.84	19	0.00	0.00	0.00	0.00	0
NRAO 190	0.31	0.08	0.31	0.31	1	0.25	0.06	0.25	0.25	1
0440+345	0.12	0.07	0.05	0.25	24	0.26	0.04	0.20	0.28	3
P 0446+11	0.30	0.06	0.24	0.41	7	0.30	0.16	0.19	0.53	4
P 0451−28	0.18	0.10	0.06	0.34	19	0.00	0.00	0.00	0.00	0
0454−234	0.87	0.19	0.50	1.47	48	0.79	0.16	0.43	0.99	13
P 0458−02	1.37	0.35	0.50	1.94	38	1.58	0.30	0.99	1.96	19
P 0458+138	0.11	0.07	0.03	0.31	26	0.20	0.06	0.17	0.25	2
GC 0459+06	0.15	0.05	0.08	0.23	11	0.23	0.06	0.23	0.23	1
0500+019	0.35	0.08	0.28	0.54	15	0.42	0.12	0.33	0.50	2
P 0502+049	0.29	0.09	0.10	0.38	13	0.33	0.08	0.33	0.33	1
0454+844	0.00	0.00	0.00	0.00	0	0.21	0.05	0.04	0.30	133
P 0506+101	0.33	0.22	0.07	0.89	49	0.20	0.06	0.09	0.33	22
P 0507+17	0.29	0.06	0.15	0.42	41	0.20	0.00	0.20	0.20	3
P 0511−220	0.55	0.08	0.41	0.63	10	0.20	0.07	0.13	0.32	9
P 0528+134	1.07	1.03	0.12	4.80	75	1.27	1.17	0.26	4.53	74
P 0537−441	2.18	0.74	0.91	3.47	27	0.00	0.00	0.00	0.00	0
P 0537−158	0.06	0.02	0.04	0.09	6	0.05	0.01	0.05	0.06	5
0536+145	0.58	0.19	0.22	0.95	62	0.68	0.22	0.23	0.99	17
0544+273	0.25	0.13	0.07	0.52	28	0.23	0.27	0.04	0.51	3
DA 193	1.68	0.36	0.85	2.70	95	2.15	0.57	1.11	3.30	130
0556+238	0.31	0.11	0.17	0.58	40	0.30	0.04	0.23	0.37	19
0600+177	0.18	0.05	0.07	0.30	59	0.22	0.05	0.16	0.28	4
P 0605−08	0.88	0.11	0.68	1.10	18	0.67	0.22	0.30	1.22	38
P 0607−15	1.68	0.55	0.58	2.46	14	1.63	0.96	0.54	4.84	25
0611+131	0.13	0.06	0.04	0.27	14	0.28	0.03	0.23	0.31	7
0615+820	0.00	0.00	0.00	0.00	0	0.16	0.07	0.02	0.29	51
3C 166	0.15	0.08	0.04	0.34	34	0.14	0.04	0.10	0.17	3
P 0646−306	0.46	0.12	0.24	0.66	24	0.00	0.00	0.00	0.00	0

Table 2 (cont'd).

Source	Goldstone–Australia baseline					Goldstone–Madrid baseline				
	$\overline{S_{corr}}$	σ_{rms}	S_{min}	S_{max}	N_{obs}	$\overline{S_{corr}}$	σ_{rms}	S_{min}	S_{max}	N_{obs}
0650+371	0.15	0.08	0.05	0.28	37	0.22	0.08	0.09	0.45	71
0657+172	0.60	0.22	0.25	1.46	80	0.56	0.19	0.23	0.90	50
OI 417	0.08	0.02	0.04	0.10	16	0.14	0.06	0.06	0.23	15
0716+714	0.00	0.00	0.00	0.00	0	0.36	0.14	0.08	0.73	42
P 0722+145	0.35	0.14	0.10	0.50	8	0.22	0.07	0.15	0.29	4
DW 0723−00	0.34	0.06	0.23	0.45	22	0.10	0.02	0.09	0.11	2
P 0727−11	1.99	0.67	0.82	3.82	92	2.16	0.86	0.79	4.21	75
P 0735+17	0.76	0.50	0.15	2.31	77	1.09	0.71	0.13	2.56	90
P 0736+01	0.72	0.08	0.58	0.94	26	0.33	0.15	0.07	0.59	26
OI 363	0.41	0.23	0.27	0.66	3	0.59	0.40	0.15	1.12	6
DW 0742+10	0.45	0.06	0.32	0.54	22	0.15	0.08	0.07	0.33	16
P 0743−006	0.31	0.20	0.03	0.70	30	0.27	0.10	0.18	0.46	10
GC 0743+25	0.11	0.06	0.02	0.20	9	0.13	0.01	0.12	0.13	2
B2 0745+24	0.42	0.25	0.06	0.84	20	0.39	0.08	0.17	0.50	42
P 0748+126	1.11	0.10	0.91	1.29	17	1.38	0.07	1.23	1.50	11
0749+540	0.00	0.00	0.00	0.00	0	0.70	0.23	0.09	1.08	55
P 0754+100	0.19	0.07	0.06	0.27	6	0.31	0.02	0.30	0.33	2
P 0805−07	0.79	0.14	0.57	1.09	24	0.45	0.15	0.19	0.74	49
P 0808+019	0.74	0.25	0.35	1.15	41	0.81	0.22	0.33	1.22	34
OJ 425	0.31	0.09	0.09	0.56	60	0.29	0.08	0.13	0.49	49
P 0823+033	0.84	0.31	0.21	1.46	88	1.03	0.28	0.46	1.63	90
B2 0827+24	0.28	0.04	0.23	0.33	7	0.50	0.21	0.14	0.67	5
OJ 448	0.00	0.00	0.00	0.00	0	0.13	0.03	0.05	0.18	23
0833+585	0.00	0.00	0.00	0.00	0	0.11	0.05	0.03	0.23	32
OJ 287	1.39	0.62	0.42	2.99	88	1.19	0.65	0.40	3.17	99
P 0859−14	0.44	0.06	0.34	0.57	20	0.32	0.10	0.20	0.51	29
OJ 499	0.23	0.05	0.14	0.27	10	0.26	0.08	0.07	0.40	46
P 0906+01	0.15	0.05	0.11	0.25	14	0.31	0.02	0.30	0.33	2
P 0912+029	0.29	0.15	0.02	0.56	12	0.00	0.00	0.00	0.00	0
0917+449	0.49	0.11	0.23	0.64	33	0.59	0.21	0.06	1.00	69
0919−260	0.15	0.06	0.07	0.25	12	0.00	0.00	0.00	0.00	0
P 0920−39	0.33	0.16	0.09	0.65	17	0.00	0.00	0.00	0.00	0
4C 39.25	1.67	0.52	0.50	2.60	85	2.79	1.23	0.84	6.05	103
P 0925−203	0.30	0.04	0.22	0.36	9	0.22	0.03	0.17	0.24	4
AO 0952+17	0.08	0.04	0.04	0.21	15	0.21	0.05	0.12	0.28	7
OK 290	0.33	0.08	0.18	0.47	48	0.46	0.18	0.10	0.89	52
GC 1004+14	0.33	0.10	0.26	0.48	7	0.33	0.04	0.28	0.37	3
1011+250	0.17	0.07	0.06	0.27	18	0.28	0.11	0.05	0.40	37
1012+232	0.29	0.21	0.06	0.66	14	0.00	0.00	0.00	0.00	0
GC 1022+19	0.26	0.03	0.23	0.32	7	0.35	0.03	0.31	0.38	6
P 1034−293	1.00	0.27	0.45	1.75	95	0.00	0.00	0.00	0.00	0
OL 064.5	0.56	0.14	0.32	0.85	14	0.49	0.04	0.43	0.57	7
3C 245	0.24	0.06	0.20	0.31	3	0.28	0.03	0.24	0.31	4

Table 2 (cont'd).

Source	Goldstone–Australia baseline					Goldstone–Madrid baseline				
	$\overline{S_{corr}}$	σ_{rms}	S_{min}	S_{max}	N_{obs}	$\overline{S_{corr}}$	σ_{rms}	S_{min}	S_{max}	N_{obs}
1039+811	0.00	0.00	0.00	0.00	0	0.66	0.25	0.08	1.05	76
P 1042+071	0.16	0.03	0.11	0.19	4	0.15	0.06	0.09	0.22	7
1044+719	0.00	0.00	0.00	0.00	0	0.54	0.22	0.08	0.82	40
P 1055+01	1.96	0.28	1.18	2.47	90	1.50	0.34	0.97	2.27	76
P 1104−445	1.00	0.25	0.48	1.66	29	0.00	0.00	0.00	0.00	0
GC 1111+14	0.25	0.04	0.19	0.31	7	0.16	0.01	0.16	0.17	2
P 1116+12	0.41	0.12	0.26	0.75	16	0.61	0.06	0.50	0.76	25
P 1123+26	0.36	0.09	0.23	0.62	62	0.29	0.10	0.10	0.55	102
P 1124−186	0.52	0.19	0.15	0.81	26	0.46	0.20	0.19	0.73	10
P 1127−14	0.29	0.08	0.13	0.38	15	0.31	0.13	0.08	0.58	43
GC 1128+38	0.40	0.12	0.20	0.54	14	0.50	0.20	0.31	0.69	3
P 1130+009	0.11	0.05	0.04	0.16	18	0.16	0.02	0.14	0.18	5
1144+402	0.55	0.11	0.34	0.72	21	0.46	0.11	0.32	0.62	12
P 1144−379	1.81	0.74	0.56	3.93	100	0.00	0.00	0.00	0.00	0
1145−071	0.17	0.07	0.08	0.26	11	0.18	0.04	0.13	0.27	10
P 1148−00	0.09	0.02	0.05	0.11	6	0.23	0.05	0.18	0.29	4
1150+812	0.00	0.00	0.00	0.00	0	0.50	0.19	0.03	0.93	84
P 1156−094	0.12	0.02	0.08	0.14	13	0.00	0.00	0.00	0.00	0
GC 1156+29	0.46	0.20	0.15	1.13	41	0.82	0.20	0.36	1.32	61
ON 231	0.13	0.08	0.04	0.29	35	0.22	0.03	0.17	0.26	13
P 1222+037	0.31	0.04	0.24	0.36	6	0.36	0.09	0.36	0.36	1
3C 273	2.40	1.04	0.34	4.31	74	2.72	1.07	0.35	6.09	70
3C 274	0.24	0.11	0.12	0.37	5	0.00	0.00	0.00	0.00	0
1243−072	0.31	0.05	0.20	0.38	8	0.27	0.04	0.21	0.33	10
P 1244−255	0.90	0.40	0.25	2.00	75	0.95	0.16	0.73	1.09	4
P 1252+11	0.19	0.09	0.05	0.34	21	0.16	0.05	0.05	0.22	22
3C 279	1.70	0.59	0.62	2.94	20	2.86	0.91	0.62	4.48	64
P 1302−102	0.27	0.14	0.04	0.56	28	0.29	0.11	0.13	0.51	38
B2 1308+32	1.77	0.39	0.67	2.48	87	1.99	0.51	0.61	2.86	108
OP−322	0.76	0.43	0.28	1.81	79	0.00	0.00	0.00	0.00	0
OP 326	0.13	0.06	0.06	0.33	28	0.31	0.06	0.21	0.42	19
1324+224	0.63	0.30	0.21	1.20	60	1.04	0.26	0.52	1.50	74
DW 1335−12	2.11	0.73	0.57	3.55	90	2.36	0.70	0.82	4.16	72
1338+381	0.04	0.01	0.03	0.05	4	0.04	0.02	0.01	0.07	11
GC 1342+662	0.00	0.00	0.00	0.00	0	0.17	0.14	0.07	0.42	8
GC 1342+663	0.00	0.00	0.00	0.00	0	0.21	0.09	0.04	0.47	95
P 1349−439	0.37	0.09	0.23	0.54	43	0.00	0.00	0.00	0.00	0
P 1354+19	0.38	0.07	0.20	0.57	80	0.25	0.07	0.09	0.46	85
OP−192	0.61	0.13	0.34	0.87	54	0.41	0.21	0.16	0.76	13
OQ 208	0.17	0.09	0.05	0.39	43	0.46	0.13	0.34	0.72	7
P 1406−076	0.42	0.15	0.13	0.60	38	0.24	0.04	0.19	0.27	4
P 1413+135	0.99	0.28	0.44	1.32	15	0.77	0.32	0.30	1.26	24
GC 1418+54	0.00	0.00	0.00	0.00	0	0.25	0.08	0.18	0.34	3

Table 2 (cont'd).

Source	Goldstone–Australia baseline					Goldstone–Madrid baseline				
	$\overline{S_{corr}}$	σ_{rms}	S_{min}	S_{max}	N_{obs}	$\overline{S_{corr}}$	σ_{rms}	S_{min}	S_{max}	N_{obs}
P 1424−41	0.87	0.48	0.15	2.18	57	0.00	0.00	0.00	0.00	0
OQ−151	0.16	0.05	0.07	0.28	30	0.11	0.10	0.05	0.23	3
P 1435−218	0.21	0.06	0.10	0.32	34	0.11	0.07	0.06	0.30	11
1443−162	0.24	0.05	0.13	0.35	31	0.17	0.07	0.11	0.26	5
P 1445−16	0.27	0.06	0.13	0.39	45	0.17	0.07	0.09	0.26	6
OR 103	0.61	0.21	0.23	1.04	90	0.48	0.26	0.03	0.79	82
1504+377	0.18	0.12	0.07	0.41	7	0.21	0.06	0.12	0.31	24
P 1504−167	0.42	0.14	0.13	0.70	63	0.48	0.19	0.12	0.86	49
P 1510−08	1.29	0.64	0.28	2.96	86	0.99	0.41	0.26	2.17	71
P 1511−100	0.23	0.13	0.05	0.50	33	0.25	0.05	0.17	0.31	8
P 1514−24	0.32	0.12	0.09	0.70	46	0.49	0.12	0.49	0.49	1
P 1519−273	1.22	0.25	0.72	1.80	82	0.00	0.00	0.00	0.00	0
P 1532+01	0.28	0.08	0.18	0.48	20	0.14	0.06	0.03	0.23	21
GC 1538+14	0.35	0.10	0.17	0.65	51	0.38	0.09	0.28	0.61	30
P 1546+027	0.30	0.09	0.22	0.51	13	0.88	0.35	0.42	1.52	36
DW 1548+05	0.44	0.17	0.31	1.11	23	0.92	0.32	0.50	1.92	45
DW 1555+00	0.75	0.15	0.39	0.98	75	0.68	0.15	0.35	1.05	71
P 1555−140	0.04	0.01	0.03	0.05	8	0.00	0.00	0.00	0.00	0
B2 1600+33	0.16	0.08	0.06	0.25	5	0.45	0.17	0.18	0.90	27
P 1604−333	0.21	0.03	0.11	0.27	43	0.00	0.00	0.00	0.00	0
P 1606+10	0.65	0.20	0.28	1.07	34	0.58	0.05	0.49	0.63	5
DA 406	0.76	0.19	0.41	1.04	21	1.42	0.38	0.19	2.43	80
P 1614+051	0.25	0.05	0.21	0.34	6	0.21	0.06	0.13	0.27	7
P 1622−253	0.70	0.34	0.27	1.38	25	0.00	0.00	0.00	0.00	0
1624+416	0.14	0.06	0.03	0.29	31	0.17	0.04	0.09	0.22	11
P 1622−29	0.79	0.27	0.16	1.34	25	0.00	0.00	0.00	0.00	0
GC 1633+38	0.30	0.10	0.12	0.39	8	0.50	0.26	0.06	0.93	90
P 1637+574	0.00	0.00	0.00	0.00	0	0.75	0.26	0.07	1.38	120
NRAO 512	0.54	0.03	0.52	0.59	4	0.62	0.22	0.23	1.15	67
1642+690	0.00	0.00	0.00	0.00	0	0.48	0.20	0.09	0.99	75
3C 345	2.27	1.24	0.35	4.49	81	2.39	1.24	0.60	4.68	84
P 1647−296	0.52	0.18	0.19	0.85	26	0.00	0.00	0.00	0.00	0
DA 426	0.28	0.06	0.14	0.37	20	0.26	0.08	0.13	0.41	11
OS 092	0.46	0.13	0.26	0.59	12	0.54	0.19	0.26	0.86	16
DW 1656+05	0.15	0.15	0.03	0.53	13	0.23	0.08	0.12	0.38	24
P 1657−261	0.99	0.39	0.35	2.15	70	1.07	0.12	0.99	1.16	2
OT−111	0.27	0.09	0.06	0.40	48	0.27	0.07	0.13	0.40	17
GC 1717+17	0.34	0.08	0.34	0.34	1	0.59	0.03	0.57	0.61	2
NRAO 530	1.77	0.96	0.70	5.74	102	1.84	0.74	1.07	5.22	69
1732+389	0.59	0.16	0.09	0.89	50	0.50	0.19	0.18	0.94	61
OT 465	0.35	0.04	0.28	0.38	5	0.42	0.22	0.04	0.76	10
4C 51.37	0.00	0.00	0.00	0.00	0	0.94	0.58	0.04	2.15	99
P 1741−038	1.16	0.54	0.13	2.44	100	1.40	0.37	0.55	2.49	79

Table 2 (cont'd).

Source	Goldstone–Australia baseline					Goldstone–Madrid baseline				
	$\overline{S_{corr}}$	σ_{rms}	S_{min}	S_{max}	N_{obs}	$\overline{S_{corr}}$	σ_{rms}	S_{min}	S_{max}	N_{obs}
GC 1743+17	0.21	0.06	0.12	0.31	14	0.40	0.05	0.24	0.51	51
OT 081	1.10	0.40	0.36	1.53	28	1.90	0.90	0.49	4.03	80
GC 1751+28	0.17	0.08	0.03	0.29	25	0.29	0.03	0.23	0.32	8
1803+784	0.00	0.00	0.00	0.00	0	1.07	0.35	0.11	1.97	112
3C 371	0.00	0.00	0.00	0.00	0	0.44	0.16	0.18	1.05	98
1826+796	0.00	0.00	0.00	0.00	0	0.12	0.05	0.03	0.21	24
P 1821+10	0.17	0.08	0.06	0.22	4	0.25	0.05	0.22	0.34	5
3C 390.3	0.00	0.00	0.00	0.00	0	0.15	0.07	0.03	0.23	12
3C 395	0.43	0.11	0.24	0.58	13	0.37	0.25	0.08	0.88	11
OV−213	0.54	0.20	0.08	0.93	84	0.80	0.23	0.37	1.15	29
OV−235	0.76	0.32	0.10	1.24	94	0.97	0.21	0.62	1.36	26
OV−236	6.27	1.92	1.01	10.81	112	0.00	0.00	0.00	0.00	0
OV 239.7	0.29	0.11	0.05	0.49	73	0.35	0.12	0.12	0.64	97
1928+738	0.00	0.00	0.00	0.00	0	0.78	0.34	0.13	1.70	90
1929+226	0.24	0.03	0.21	0.28	5	0.27	0.06	0.19	0.36	18
P 1933−400	0.37	0.13	0.07	0.58	74	0.00	0.00	0.00	0.00	0
P 1936−15	0.77	0.23	0.17	1.28	45	0.56	0.18	0.34	0.74	4
1947+079	0.13	0.01	0.11	0.15	14	0.08	0.02	0.06	0.10	8
1954+513	0.00	0.00	0.00	0.00	0	0.56	0.27	0.06	1.43	91
1955+335	0.00	0.00	0.00	0.00	0	0.10	0.05	0.06	0.14	1
OV−198	0.98	0.64	0.08	2.73	101	0.79	0.39	0.10	1.86	48
OW−015	0.05	0.01	0.03	0.07	20	0.00	0.00	0.00	0.00	0
P 2008−159	0.53	0.16	0.12	0.75	50	0.78	0.18	0.38	1.07	21
2017+743	0.00	0.00	0.00	0.00	0	0.20	0.06	0.09	0.31	36
OW 637	0.00	0.00	0.00	0.00	0	0.72	0.27	0.08	1.40	61
2021+317	0.12	0.04	0.09	0.18	4	0.48	0.18	0.23	0.89	31
OW 551	0.00	0.00	0.00	0.00	0	0.12	0.07	0.05	0.19	3
P 2029+121	0.26	0.03	0.24	0.30	3	0.30	0.04	0.27	0.32	2
3C 418	0.00	0.00	0.00	0.00	0	0.91	0.19	0.60	1.26	35
2051+745	0.00	0.00	0.00	0.00	0	0.09	0.06	0.02	0.22	22
2100+468	0.00	0.00	0.00	0.00	0	0.03	0.02	0.02	0.06	6
P 2106−413	1.02	0.15	0.75	1.32	22	0.00	0.00	0.00	0.00	0
B2 2113+29B	0.32	0.01	0.30	0.33	4	0.56	0.21	0.26	0.94	35
OX 036	0.29	0.15	0.04	0.66	45	0.25	0.13	0.08	0.48	13
P 2126−15	0.15	0.05	0.08	0.27	23	0.34	0.09	0.16	0.47	12
P 2127+04	0.03	0.01	0.03	0.05	7	0.06	0.05	0.03	0.19	8
P 2128−12	0.37	0.22	0.10	1.09	45	0.40	0.18	0.13	0.77	23
P 2131−021	0.92	0.35	0.07	1.41	73	0.67	0.32	0.05	1.15	57
P 2134+004	0.87	0.25	0.16	1.43	85	1.33	0.25	0.74	1.86	62
OX 161	1.29	0.15	1.04	1.47	8	1.16	0.08	1.03	1.36	14
OX−173	0.20	0.07	0.08	0.31	25	0.26	0.07	0.11	0.35	11
OX 074	0.32	0.11	0.21	0.58	14	0.28	0.08	0.18	0.40	7
P 2145+06	3.55	0.70	0.59	4.88	71	2.64	0.48	1.15	3.94	70

Table 2 (cont'd).

Source	Goldstone–Australia baseline					Goldstone–Madrid baseline				
	$\overline{S_{corr}}$	σ_{rms}	S_{min}	S_{max}	N_{obs}	$\overline{S_{corr}}$	σ_{rms}	S_{min}	S_{max}	N_{obs}
OX 082	0.22	0.04	0.13	0.31	36	0.20	0.05	0.13	0.25	7
2150+173	0.16	0.05	0.07	0.25	11	0.19	0.03	0.06	0.21	23
OX−192	0.62	0.14	0.39	0.94	37	0.29	0.10	0.09	0.50	33
VRO 42.22.01	0.53	0.24	0.10	1.31	65	1.02	0.47	0.19	2.62	112
B2 2201+31A	0.29	0.10	0.10	0.49	32	0.84	0.32	0.21	1.55	33
P 2216−03	0.43	0.11	0.12	0.65	49	0.76	0.25	0.37	1.22	32
3C 446	1.77	0.76	0.43	3.50	46	0.99	0.60	0.29	2.36	27
P 2227−08	0.70	0.44	0.03	1.60	60	0.48	0.28	0.21	1.09	19
2229+695	0.00	0.00	0.00	0.00	0	0.12	0.10	0.03	0.41	27
CTA 102	0.67	0.20	0.10	1.26	75	0.62	0.26	0.25	1.36	67
GC 2234+28	0.49	0.17	0.16	0.85	67	0.53	0.17	0.17	0.90	69
P 2233−148	0.13	0.05	0.06	0.22	24	0.13	0.05	0.07	0.26	11
OY−172.6	0.65	0.30	0.08	1.38	84	1.30	0.29	0.51	1.87	56
P 2245−328	0.17	0.09	0.03	0.37	85	0.00	0.00	0.00	0.00	0
3C 454.3	2.77	1.70	0.39	6.96	71	2.28	1.63	0.22	6.54	51
P 2252−089	0.12	0.05	0.03	0.24	26	0.08	0.03	0.04	0.14	9
GC 2253+41	0.14	0.03	0.08	0.21	26	0.00	0.00	0.00	0.00	0
GC 2254+07	0.10	0.05	0.05	0.22	20	0.11	0.06	0.08	0.22	10
P 2254+024	0.20	0.04	0.12	0.28	29	0.21	0.04	0.17	0.27	7
P 2255−282	1.15	0.48	0.75	2.39	49	0.00	0.00	0.00	0.00	0
GC 2318+04	0.45	0.13	0.15	0.65	43	0.52	0.12	0.33	0.72	20
B2 2319+27	0.08	0.04	0.04	0.13	4	0.16	0.06	0.06	0.29	20
P 2320−035	0.28	0.07	0.04	0.37	58	0.33	0.05	0.12	0.44	48
P 2328+10	0.29	0.07	0.14	0.40	23	0.40	0.02	0.38	0.43	7
2331−240	0.51	0.10	0.26	0.68	42	0.19	0.05	0.13	0.29	11
P 2335−027	0.17	0.07	0.05	0.28	28	0.18	0.05	0.07	0.27	22
P 2344+09	0.28	0.11	0.07	0.44	23	0.24	0.04	0.21	0.28	3
P 2345−16	0.90	0.41	0.03	1.66	78	0.36	0.28	0.07	0.98	44
2351+456	0.26	0.08	0.15	0.47	17	0.22	0.09	0.06	0.41	26
2351−154	0.53	0.15	0.20	0.84	41	0.37	0.14	0.20	0.71	24
DA 611	0.00	0.00	0.00	0.00	0	0.06	0.02	0.06	0.06	1
P 2355−106	0.70	0.22	0.18	1.11	64	0.43	0.16	0.29	0.91	25

Table 3. Total flux densities.

Source	X-band (8.4 GHz)					S-band (2.3 GHz)				
	$\overline{S_{tot}}$	σ_{rms}	S_{min}	S_{max}	N_{obs}	$\overline{S_{tot}}$	σ_{rms}	S_{min}	S_{max}	N_{obs}
0003−066	2.02	0.62	1.03	2.90	9	0.00	0.00	0.00	0.00	0
0016+731	1.29	0.49	0.70	1.47	3	0.00	0.00	0.00	0.00	0
P 0048−09	1.24	0.19	1.24	1.24	1	0.00	0.00	0.00	0.00	0
P 0104−408	3.73	0.56	3.73	3.73	1	0.00	0.00	0.00	0.00	0
P 0106+01	1.38	0.31	1.03	1.73	7	1.73	0.26	1.73	1.73	1
P 0112−017	0.82	0.39	0.41	1.23	4	0.00	0.00	0.00	0.00	0
P 0113−118	1.58	0.25	1.56	1.66	2	0.00	0.00	0.00	0.00	0
P 0119+11	1.09	0.59	0.88	1.86	5	0.00	0.00	0.00	0.00	0
GC 0119+04	1.18	0.52	0.62	1.86	5	0.00	0.00	0.00	0.00	0
DA 55	1.20	1.06	0.62	3.49	7	0.00	0.00	0.00	0.00	0
0146+056	1.44	0.22	1.44	1.44	1	0.00	0.00	0.00	0.00	0
0159+723	0.00	0.00	0.00	0.00	0	3.16	0.47	3.16	3.16	1
P 0201+113	0.00	0.00	0.00	0.00	0	2.37	0.36	2.37	2.37	1
P 0202+14	2.41	1.22	1.65	6.36	17	3.89	1.28	3.07	5.88	5
DW 0202+31	1.48	2.14	0.37	3.29	2	0.00	0.00	0.00	0.00	0
P 0208−512	3.95	0.66	3.77	4.18	2	0.00	0.00	0.00	0.00	0
0212+735	2.25	0.92	0.62	3.65	24	1.71	0.59	1.34	2.09	2
GC 0221+06	2.02	0.90	1.45	2.65	2	0.00	0.00	0.00	0.00	0
P 0229+13	1.16	0.31	0.90	1.48	4	0.00	0.00	0.00	0.00	0
CTD 20	2.65	0.70	1.64	3.55	24	4.02	2.04	2.57	6.68	4
GC 0235+16	2.09	1.79	0.70	5.42	7	0.00	0.00	0.00	0.00	0
GC 0237+04	0.99	0.31	0.70	1.24	3	0.00	0.00	0.00	0.00	0
P 0237−23	2.05	0.72	0.70	2.49	7	3.98	0.60	3.98	3.98	1
OD 166	1.23	0.91	0.82	2.61	4	1.58	0.24	1.58	1.58	1
OE 400	1.15	0.80	0.62	2.06	3	0.99	0.15	0.99	0.99	1
0306+102	0.70	0.10	0.70	0.70	1	0.00	0.00	0.00	0.00	0
0309+411	0.62	0.09	0.62	0.62	1	0.00	0.00	0.00	0.00	0
3C 84	23.89	4.81	19.30	28.84	10	23.93	16.49	21.26	46.43	3
0326+277	0.37	0.06	0.37	0.37	1	0.00	0.00	0.00	0.00	0
P 0332−403	1.94	0.29	1.94	1.94	1	0.00	0.00	0.00	0.00	0
NRAO 140	1.48	0.34	1.26	1.77	3	0.00	0.00	0.00	0.00	0
CTA 26	2.82	0.76	1.66	3.91	9	0.00	0.00	0.00	0.00	0
0342+147	0.74	0.11	0.74	0.74	1	0.00	0.00	0.00	0.00	0
CTD 26	0.58	0.17	0.41	0.70	3	0.00	0.00	0.00	0.00	0
P 0402−362	2.39	0.61	1.85	3.31	7	0.00	0.00	0.00	0.00	0
P 0420−01	2.65	1.01	1.04	4.56	27	3.28	2.71	2.32	7.72	4
P 0425+048	0.74	0.11	0.74	0.74	1	0.00	0.00	0.00	0.00	0
3C 120	6.17	0.93	6.17	6.17	1	0.00	0.00	0.00	0.00	0
P 0434−188	0.74	0.11	0.74	0.74	1	0.00	0.00	0.00	0.00	0
P 0438−43	3.24	0.56	2.89	3.51	4	0.00	0.00	0.00	0.00	0
P 0451−28	1.86	0.28	1.86	1.86	1	0.00	0.00	0.00	0.00	0
0454−234	2.05	0.31	2.05	2.05	1	0.00	0.00	0.00	0.00	0
P 0458−02	2.50	0.67	1.65	3.29	7	0.00	0.00	0.00	0.00	0

Table 3 (cont'd).

Source	X-band (8.4 GHz)					S-band (2.3 GHz)				
	$\overline{S_{tot}}$	σ_{rms}	S_{min}	S_{max}	N_{obs}	$\overline{S_{tot}}$	σ_{rms}	S_{min}	S_{max}	N_{obs}
0500+019	1.44	0.22	1.44	1.44	1	0.00	0.00	0.00	0.00	0
0454+844	0.39	0.32	0.36	0.70	2	0.00	0.00	0.00	0.00	0
P 0528+134	1.91	1.12	0.82	4.86	12	3.73	0.56	3.73	3.73	1
P 0537−441	4.46	0.76	3.93	5.02	6	0.00	0.00	0.00	0.00	0
DA 193	5.01	1.52	2.87	10.17	51	3.76	0.77	3.06	4.67	7
0556+238	1.24	0.19	1.24	1.24	1	0.00	0.00	0.00	0.00	0
P 0605−08	2.63	0.55	1.84	3.31	11	0.00	0.00	0.00	0.00	0
P 0607−15	7.95	1.19	7.95	7.95	1	7.06	1.06	7.06	7.06	1
0615+820	0.71	0.14	0.62	0.73	3	0.00	0.00	0.00	0.00	0
P 0637−75	7.39	1.32	6.62	8.23	4	0.00	0.00	0.00	0.00	0
0650+371	0.61	3.11	0.45	5.00	3	0.84	0.13	0.84	0.84	1
0657+172	1.44	0.27	1.23	1.64	4	4.59	5.86	3.81	10.36	2
OI 417	0.88	0.35	0.66	1.11	2	0.00	0.00	0.00	0.00	0
DW 0723−00	1.43	0.27	1.26	1.65	4	0.00	0.00	0.00	0.00	0
P 0727−11	4.47	1.83	2.22	8.22	27	3.89	2.16	2.39	7.88	7
P 0735+17	2.96	0.89	2.05	4.72	27	3.22	1.26	2.49	4.69	3
P 0736+01	1.48	0.22	1.48	1.48	1	0.00	0.00	0.00	0.00	0
OI 363	2.13	0.32	2.13	2.13	1	0.00	0.00	0.00	0.00	0
DW 0742+10	2.83	0.48	2.59	3.04	3	0.00	0.00	0.00	0.00	0
P 0743−006	1.85	0.36	1.65	1.97	2	0.00	0.00	0.00	0.00	0
B2 0745+24	0.74	0.11	0.74	0.74	1	0.00	0.00	0.00	0.00	0
P 0748+126	2.47	0.37	2.47	2.47	1	0.00	0.00	0.00	0.00	0
0749+540	1.74	1.38	0.99	3.50	3	0.00	0.00	0.00	0.00	0
P 0805−07	1.62	0.24	1.62	1.62	1	0.00	0.00	0.00	0.00	0
P 0808+019	1.18	0.20	1.11	1.26	2	4.24	0.64	4.24	4.24	1
OJ 425	1.16	0.17	1.16	1.16	1	0.00	0.00	0.00	0.00	0
P 0823+033	1.56	1.03	0.83	4.73	19	2.03	0.52	1.58	2.68	5
0833+585	0.37	0.06	0.37	0.37	1	0.00	0.00	0.00	0.00	0
OJ 287	2.63	1.02	1.84	5.49	30	2.92	0.77	2.52	3.70	3
P 0859−14	1.98	0.34	1.86	2.27	5	0.00	0.00	0.00	0.00	0
OJ 499	0.68	0.39	0.41	0.95	2	2.83	5.94	2.06	8.71	2
P 0906+01	1.19	0.70	1.08	1.86	2	0.00	0.00	0.00	0.00	0
P 0912+029	0.78	3.16	0.65	3.93	2	0.00	0.00	0.00	0.00	0
0917+449	1.43	0.37	0.95	1.81	8	0.00	0.00	0.00	0.00	0
OK−232	2.49	0.51	2.07	3.10	6	0.00	0.00	0.00	0.00	0
P 0920−39	1.03	0.15	1.03	1.03	1	0.00	0.00	0.00	0.00	0
4C 39.25	8.17	2.94	5.33	18.38	52	4.86	1.43	3.61	7.46	9
OK 290	1.12	0.46	0.41	1.69	11	0.00	0.00	0.00	0.00	0
1011+250	0.98	0.16	0.97	1.04	2	0.00	0.00	0.00	0.00	0
P 1034−293	1.31	0.47	0.96	2.24	9	0.00	0.00	0.00	0.00	0
3C 245	0.94	0.14	0.94	0.94	1	0.00	0.00	0.00	0.00	0
1039+811	1.28	0.26	1.03	1.44	4	0.00	0.00	0.00	0.00	0
1044+719	0.96	0.41	0.70	1.24	2	1.21	0.41	0.79	1.58	4

Table 3 (cont'd).

Source	X-band (8.4 GHz)					S-band (2.3 GHz)				
	$\overline{S_{tot}}$	σ_{rms}	S_{min}	S_{max}	N_{obs}	$\overline{S_{tot}}$	σ_{rms}	S_{min}	S_{max}	N_{obs}
P 1055+01	3.06	0.83	1.45	4.43	33	3.55	1.37	2.22	6.65	10
P 1057−79	2.92	0.44	2.92	2.92	1	0.00	0.00	0.00	0.00	0
P 1104−445	3.76	0.63	3.35	4.13	6	0.00	0.00	0.00	0.00	0
P 1123+26	1.04	0.26	0.74	1.30	7	1.67	0.66	1.24	2.11	2
P 1127−14	2.60	0.80	1.79	3.72	9	6.81	1.02	6.81	6.81	1
GC 1128+38	1.14	0.22	1.12	1.27	2	0.00	0.00	0.00	0.00	0
P 1143−245	1.17	0.19	1.15	1.24	2	0.00	0.00	0.00	0.00	0
1144+402	0.76	0.23	0.62	0.91	2	0.54	0.08	0.54	0.54	1
P 1144−379	2.58	0.84	2.06	4.12	10	2.57	0.39	2.57	2.57	1
1150+812	1.40	0.21	1.40	1.40	1	2.25	9.38	1.58	11.61	2
GC 1156+29	1.46	0.52	0.62	2.15	7	2.36	0.55	2.07	2.67	2
3C 273	29.50	8.70	21.05	48.17	37	51.26	8.46	46.90	57.39	8
3C 274	7.76	1.16	7.76	7.76	1	0.00	0.00	0.00	0.00	0
P 1244−255	1.97	0.47	1.66	2.48	7	0.00	0.00	0.00	0.00	0
3C 279	9.09	2.83	6.25	14.65	15	4.06	7.81	1.83	13.05	5
B2 1308+32	2.49	0.85	1.44	4.68	30	2.81	1.59	1.18	5.37	6
OP−322	1.03	0.15	1.03	1.03	1	0.00	0.00	0.00	0.00	0
OP 326	4.19	0.63	4.19	4.19	1	0.00	0.00	0.00	0.00	0
1324+224	1.21	0.38	0.82	1.77	7	1.24	0.19	1.24	1.24	1
DW 1335−12	3.40	1.64	2.28	8.67	22	0.00	0.00	0.00	0.00	0
GC 1342+663	0.70	0.10	0.70	0.70	1	0.00	0.00	0.00	0.00	0
P 1354+19	1.34	0.45	0.62	1.91	10	3.15	0.47	3.15	3.15	1
OP−192	1.68	0.89	0.83	2.89	4	0.00	0.00	0.00	0.00	0
OQ 208	1.69	0.37	1.32	1.93	5	0.00	0.00	0.00	0.00	0
P 1424−41	2.63	1.09	2.07	3.95	3	0.00	0.00	0.00	0.00	0
OR 103	1.36	0.65	0.41	2.07	7	2.02	0.30	2.02	2.02	1
P 1504−167	1.83	0.42	1.53	2.35	5	3.98	0.60	3.98	3.98	1
P 1510−08	2.46	0.73	2.05	4.15	10	2.12	0.70	1.69	2.57	2
P 1519−273	1.96	0.76	1.24	2.70	4	0.00	0.00	0.00	0.00	0
DW 1548+05	1.33	0.61	0.62	2.02	4	0.00	0.00	0.00	0.00	0
DW 1555+00	1.28	0.49	0.62	1.74	8	0.00	0.00	0.00	0.00	0
B2 1600+33	1.85	0.28	1.85	1.85	1	0.00	0.00	0.00	0.00	0
P 1606+10	1.64	0.25	1.64	1.64	1	0.00	0.00	0.00	0.00	0
DA 406	2.34	0.76	1.65	3.93	20	3.69	0.55	3.69	3.69	1
P 1614+051	0.51	0.08	0.51	0.51	1	0.00	0.00	0.00	0.00	0
P 1610−77	3.67	0.67	3.44	4.37	5	0.00	0.00	0.00	0.00	0
P 1622−253	2.17	0.33	2.17	2.17	1	0.00	0.00	0.00	0.00	0
P 1622−29	2.47	0.37	2.46	2.48	2	0.00	0.00	0.00	0.00	0
GC 1633+38	1.90	1.03	0.82	4.95	13	3.95	0.59	3.95	3.95	1
P 1637+574	1.16	0.43	0.62	1.73	6	2.04	2.90	0.89	4.69	2
NRAO 512	1.48	0.86	0.62	2.88	5	0.00	0.00	0.00	0.00	0
1642+690	0.89	0.39	0.78	1.44	5	2.07	0.31	2.07	2.07	1
3C 345	4.79	2.44	3.49	9.39	17	0.00	0.00	0.00	0.00	0

Table 3 (cont'd).

Source	X-band (8.4 GHz)					S-band (2.3 GHz)				
	$\overline{S_{tot}}$	σ_{rms}	S_{min}	S_{max}	N_{obs}	$\overline{S_{tot}}$	σ_{rms}	S_{min}	S_{max}	N_{obs}
DA 426	1.15	0.29	0.99	1.31	2	0.00	0.00	0.00	0.00	0
OS 092	1.03	0.15	1.03	1.03	1	5.87	0.88	5.87	5.87	1
DW 1656+05	0.79	0.12	0.79	0.79	1	0.00	0.00	0.00	0.00	0
P 1657−261	1.74	1.11	0.86	3.48	8	0.00	0.00	0.00	0.00	0
NRAO 530	4.05	1.71	1.88	6.82	33	7.54	1.27	6.99	8.45	5
1732+389	0.88	0.37	0.41	1.24	7	0.00	0.00	0.00	0.00	0
OT 465	1.03	0.15	1.03	1.03	1	0.00	0.00	0.00	0.00	0
4C 51.37	1.82	0.77	0.62	2.94	11	0.00	0.00	0.00	0.00	0
P 1741−038	2.13	0.63	1.04	3.32	24	2.28	0.34	2.28	2.28	1
GC 1743+17	0.77	0.20	0.41	0.80	6	0.00	0.00	0.00	0.00	0
OT 081	2.11	1.00	1.03	4.23	8	0.89	0.13	0.89	0.89	1
1803+784	1.98	0.65	1.24	3.05	21	2.65	0.73	2.08	3.95	9
3C 371	1.43	0.59	0.70	2.10	8	2.96	0.44	2.96	2.96	1
3C 390.3	1.65	0.25	1.65	1.65	2	9.12	1.37	9.12	9.12	1
OV−213	2.35	0.61	1.63	3.29	8	5.48	0.82	5.48	5.48	1
OV−235	2.71	0.59	2.10	3.55	9	0.00	0.00	0.00	0.00	0
OV−236	14.26	2.59	12.81	17.69	17	12.47	2.39	10.71	14.05	4
OV 239.7	1.26	0.51	0.82	2.38	13	2.52	4.49	1.63	6.91	2
1928+738	2.75	0.83	1.65	3.72	13	4.68	1.29	4.15	7.58	9
1929+226	0.41	0.24	0.38	0.75	3	0.00	0.00	0.00	0.00	0
P 1933−400	0.83	0.12	0.83	0.83	1	0.00	0.00	0.00	0.00	0
P 1936−15	1.25	0.29	1.03	1.50	5	0.00	0.00	0.00	0.00	0
1947+079	0.71	0.15	0.58	0.77	4	0.00	0.00	0.00	0.00	0
1951+355	0.45	0.12	0.42	0.62	4	0.00	0.00	0.00	0.00	0
1954+513	1.22	0.53	0.41	1.88	9	0.94	0.14	0.94	0.94	1
OV−198	2.30	0.57	1.86	3.14	11	0.00	0.00	0.00	0.00	0
P 2008−159	1.34	0.37	1.03	1.65	3	0.00	0.00	0.00	0.00	0
OW 637	2.23	0.60	1.45	2.87	7	3.76	0.56	3.76	3.76	1
2021+317	1.99	0.71	1.64	2.76	3	0.00	0.00	0.00	0.00	0
P 2029+121	0.70	0.11	0.70	0.70	2	0.00	0.00	0.00	0.00	0
3C 418	1.87	0.39	1.67	2.06	2	0.00	0.00	0.00	0.00	0
2051+745	0.00	0.00	0.00	0.00	0	7.78	1.17	7.78	7.78	1
B2 2113+29B	0.86	0.29	0.59	1.16	4	6.36	0.95	6.36	6.36	1
OX 036	1.60	0.72	0.62	2.25	6	0.00	0.00	0.00	0.00	0
P 2126−15	1.74	0.26	1.74	1.74	1	0.00	0.00	0.00	0.00	0
P 2127+04	1.24	0.19	1.24	1.24	1	0.00	0.00	0.00	0.00	0
P 2128−12	2.69	0.70	2.06	3.44	5	22.08	3.31	22.08	22.08	1
P 2131−021	1.47	0.62	0.62	2.08	9	1.92	0.51	1.63	2.23	2
P 2134+004	5.55	1.45	3.91	8.24	24	6.93	2.13	5.98	9.39	3
OX−173	0.33	0.05	0.33	0.33	1	0.00	0.00	0.00	0.00	0
P 2145+06	4.82	1.49	3.30	7.19	22	3.64	3.65	2.91	7.17	2
2152−699	7.46	1.61	6.51	8.90	4	0.00	0.00	0.00	0.00	0
OX−192	2.41	0.38	2.27	2.50	4	2.67	0.40	2.67	2.67	1

Table 3 (cont'd).

Source	X-band (8.4 GHz)					S-band (2.3 GHz)				
	$\overline{S_{tot}}$	σ_{rms}	S_{min}	S_{max}	N_{obs}	$\overline{S_{tot}}$	σ_{rms}	S_{min}	S_{max}	N_{obs}
VRO 42.22.01	1.89	0.84	0.82	3.88	28	0.00	0.00	0.00	0.00	0
B2 2201+31A	2.33	0.57	1.71	2.88	11	3.81	0.57	3.81	3.81	1
P 2216−03	2.02	0.54	1.45	2.47	4	2.27	0.34	2.27	2.27	1
3C 446	4.21	1.18	2.94	5.99	10	0.00	0.00	0.00	0.00	0
P 2227−08	2.64	0.40	2.64	2.64	1	0.00	0.00	0.00	0.00	0
CTA 102	2.63	0.84	1.23	4.11	21	5.67	0.85	5.67	5.67	1
GC 2234+28	1.19	0.43	0.49	1.68	15	0.00	0.00	0.00	0.00	0
OY−172.6	2.47	0.59	1.84	3.30	10	0.00	0.00	0.00	0.00	0
3C 454.3	5.61	2.08	3.91	10.20	22	0.00	0.00	0.00	0.00	0
P 2255−282	2.48	0.74	2.08	2.98	2	0.00	0.00	0.00	0.00	0
GC 2318+04	0.90	0.13	0.90	0.90	1	0.00	0.00	0.00	0.00	0
B2 2319+27	0.41	0.06	0.41	0.41	1	3.70	0.56	3.70	3.70	1
P 2320−035	0.83	0.44	0.41	0.88	2	0.00	0.00	0.00	0.00	0
P 2326−477	2.35	0.36	2.28	2.40	2	0.00	0.00	0.00	0.00	0
P 2328+10	0.66	0.10	0.66	0.66	1	0.00	0.00	0.00	0.00	0
2331−240	0.99	0.28	0.82	1.16	2	0.00	0.00	0.00	0.00	0
P 2345−16	1.58	0.40	1.24	1.86	3	7.56	1.13	7.56	7.56	1
2351+456	0.74	0.11	0.74	0.74	1	0.00	0.00	0.00	0.00	0